South African Journal of Botany 172 (2024) 515–528

Contents lists available at ScienceDirect

South African Journal of Botany

journal homepage: www.elsevier.com/locate/sajb

# Proteome profiling of lumichrome-treated *Arabidopsis thaliana* suggests that various regulatory mechanisms mediate enhanced photosynthesis and plant growth

Motlalepula Pholo-Tait[a,1], Waltraud X. Schulze[b], Saleh Alseekh[c], Alex J. Valentine[d], Nicholas C. Le Maitre[a], James R. Lloyd[a], Jens Kossmann[a], Paul N. Hills[a,*]

[a] Institute for Plant Biotechnology, Department of Genetics, Stellenbosch University, Stellenbosch, South Africa
[b] Department of Plant Systems Biology, University of Hohenheim, Stuttgart, Germany
[c] Max Planck Institute for Molecular Plant Physiology, Potsdam-Golm, Germany
[d] Department of Botany and Zoology, University of Stellenbosch, Stellenbosch, South Africa

ARTICLE INFO

*Article History:*
Received 13 March 2024
Revised 12 July 2024
Accepted 17 July 2024
Available online 3 August 2024

Edited by: K. Dolezal

*Keywords:*
*Arabidopsis thaliana*
Proteomics
Soluble sugars
Photosynthesis
Carbon metabolism

ABSTRACT

Lumichrome, a novel bacterial molecule derived from *Sinorhizobium meliloti,* plays a crucial role in enhancing plant growth, particularly by increasing photosynthesis and influencing carbon metabolism. Through its impact on gene expression, it has been found to promote turgor-driven growth and ethylene-related delay leaf senescence. In line with previous studies, the current study revealed that treating *Arabidopsis thaliana* with lumichrome suggested the activation of jasmonate-related signals that delayed leaf senescence. Decreased AOC2 levels, together with the high levels of ABR protein, suggested delayed light and dark-induced leaf senescence. This, along with an increase in chlorophyll content, may possibly be attributed to the enhancement of optimal light absorption, energy conversion, and electron transfer capacity of active PSII reactions. In addition, the increased expression of MPH2 and ATPD subunits might have contributed to a better PSII repair, maintenance of proper photosynthetic function under changing light, and increased ATP synthase activity, ultimately resulting in higher photosynthesis efficiency. Moreover, the increased expression of TRX-M1, TRX-M4, plastid PRX-IIE, and cytosolic APX1 proteins could have improved the ability of treated plants to counteract ROS at PSII and PSI, leading to a better $CO_2$ assimilation rate and plant growth. Subsequently, increased FBA8 could have directed the fixed carbon partitioning into the cytosolic glycolysis pathway. Altogether, these changes may have contributed to increased growth through higher levels of sucrose and reducing sugars.



## 1. Introduction

Whilst the roles of phytohormones in growth, plant productivity, defence, and signalling for plant–animal–microbe interactions are well understood, a variety of non-phytohormone plant growth regulating molecules are produced by rhizosphere microorganisms, the activities of which are considerably less well understood. Amongst these is the inter-kingdom signalling metabolite, lumichrome (Phillips et al., 1999). Lumichrome (*7,8-dimethylalloxazine*) was identified from filtrates of *Sinorhizobium meliloti* cultures as a signalling molecule between the growth-promoting rhizobacterium and its host plants ((Phillips et al., 1999). It is a degradation product of riboflavin, generated by photochemical or enzymatic cleavage of the ribityl group of riboflavin under neutral or acidic conditions in the presence of sunlight (Khan et al., 2008; Phillips et al., 1999). According to a previous study (Phillips et al., 1999), applying purified lumichrome from *S. meliloti* exudates to the roots of alfalfa seedlings resulted in increased root respiration and promoted plant growth. The enhanced plant growth was attributed to increased net C assimilation, possibly via PEP carboxylase activity. However, subsequent studies reported differing effects depending on the plant species and metabolite concentrations tested.

When 10 nM purified lumichrome and 10 mL of infective rhizobial cells were applied to cowpea, bambara groundnut, soybean, pea, lupin, sorghum, and maise plants, it was observed that stomatal conductance and leaf transpiration rates were increased in cowpea. However, in bambara groundnut, soybean, and maize, both

* Corresponding author at: Institute for Plant Biotechnology, Department of Genetics, Stellenbosch University, Private Bag X1, Matieland 7602 Stellenbosch, South Africa.
*E-mail address:* phills@sun.ac.za (P.N. Hills).
[1] Current address: Centre for Bioeconomy, Faculty of Research and graduate Studies, Botswana University of Agriculture and Natural Resources, Gabarone, Botswana.

https://doi.org/10.1016/j.sajb.2024.07.036

parameters were decreased, while no significant effect was observed in pea and sorghum (Matiru and Dakora., 2005). Another study observed that 50 nM lumichrome treatment inhibited root development in cowpeas, while it did not affect other species. In addition, it depressed the development of unifoliate leaves in soybeans, the second trifoliate leaf in cowpeas, and shoot biomass in soybeans (Matiru and Dakora, 2005). However, the 5 nM of lumichrome treatment to roots of cowpea and soybean seedlings elicited early initiation of trifoliate leaf development, expansion in unifoliate and trifoliate leaves, and increased stem elongation, which together caused an increase in shoot and plant total biomass. Similarly, the 5 nM lumichrome application expanded the leaf area in maize, sorghum, lotus, and tomato (Gouws et al., 2012; Matiru and Dakora, 2005).

Enhanced growth is attributed to xylem transport and *in situ* accumulation of lumichrome in leaves. This subsequently triggers events that promote cell division and leaf expansion in both monocots and dicots (Matiru and Dakora., 2005). A transcriptomic study on *A. thaliana* supported this. When 5 nM lumichrome was applied to *A. thaliana*, it led to the overexpression of *XYLOGLUCAN ENDOTRANSGLUCOSYLASE/HYDROLASE 9 (XTH9) and EXPANSIN A4 (EXPA4)*. In addition, there was an increase in the expression of mitotic *CYCLIN A1;1 (CYCA1;1), CYCLIN D3;3 (CYCD3;3), SPIRAL 1-LIKE3 (SP1L3), RADIALLY SWOLLEN 7 (RSW7)*, and *PROTODERMAL FACTOR 1 (PDF1)* transcripts. These suggested that enhanced plant growth could be attributed to genes impacting turgor-driven growth and the mitotic cell cycle that ensures the integration of cell division and the expansion of developing leaves (Pholo et al., 2018).

Given the various previous reports, we hypothesised that lumichrome enhances photosynthesis and carbon metabolism through an array of physiological, biochemical and molecular processes, and that these responses are species dependent. Chloroplasts are the central site of photosynthesis, and photosynthesis activity is tightly linked to chloroplast development. Photosynthetic competence depends on proper chloroplast biogenesis, a complicated multistage molecular process that leads to fully differentiated and functionally mature plastids. (Skotnicová et al., 2023). Upon illumination, during natural photomorphogenesis, proplastids develop a thylakoid network and photosynthetic capacity (Pogson and Albrecht, 2011). Chloroplasts possess a thylakoid membrane network, which hosts protein complexes that carry out the light reactions of oxygenic photosynthesis and provide a medium for energy transduction (Leister, 2003; Sakamoto et al., 2008). These proteins include four multi-subunit protein complexes of the photosystem I [PSI], photosystem II [PSII], ATP synthase, and cytochrome b6f complexes, which are responsible for the primary reactions of photosynthesis (Rast et al., 2015; Wollman et al., 1999; Zhu et al., 2022).

The onset of photosynthesis is characterised by an increase in the expression of most of the nuclear genes encoding chloroplast proteins during leaf development. A variegated *A. thaliana* mutant with disrupted chloroplast development has shown impaired chloroplast-to-nucleus signalling (Dogra et al., 2019), followed by inhibited cell differentiation, leading to pleiotropic growth phenotypes (Kato et al., 2009; Næsted et al., 2004; Sakamoto et al., 2002). This signifies that the highly flexible regulation of photosynthetic light reactions in plant chloroplasts and retrograde signalling in proplastid-to-chloroplast differentiation are prerequisites to providing sufficient energy flow to downstream metabolism and plant growth.

Despite numerous reports on the importance of lumichrome for photosynthesis and plant growth, the mode of action responsible for enhancing photosynthesis and carbon metabolism, particularly at the proteomic level, still needs to be determined. Proteomics and metabolomics studies were conducted in lumichrome-treated *A. thaliana* plants to elucidate the photosynthetic, carbon metabolism, and growth-related control mechanisms.

## 2. Materials and methods

### 2.1. Plant material, growth conditions and photosynthesis-related parameters

*A. thaliana* (ecotype Columbia-0) was grown in a controlled growth cabinet with a 16/8 h day/night photoperiod at 22 ± 2 °C and 75 % relative humidity. Pots were arranged in a factorial, completely randomised block design comprising six replications and blocks. The 100 $\mu$M lumichrome stock solutions were freshly prepared by dissolving lumichrome powder (Sigma-Aldrich, USA;103217) in methanol and 1 M HCl at the ratio of 49:1 followed by stirring for at least 2 h and stored at −20 °C for 24–48 h before using once and discarding (Phillips et al., 1999). The 5 nM lumichrome working stock was prepared from the stock solution by diluting it with double-deionised water (dd$H_2O$). The control solution was prepared using the same amounts of methanol/1 M HCl (49:1) and dd$H_2O$ as the lumichrome-treated plants. Plants were treated with either 50 mL of 5 nM lumichrome or control solution for three consecutive weeks, via root drenching and foliar applications. After that, plants were given 100 mL at each treatment for the remaining experimental period. Lumichrome applications were initially given twice a week; however, the frequency changed to 3 times a week from the third week as the plant growth rate progressed.

All the data were collected from 5-week-old *A. thaliana* rosette leaves. Photosynthetic parameters were concurrently measured with an open-system photosynthesis meter (LI-COR 6400, LI-COR Inc., Lincoln, NE, USA) equipped with a standard leaf chamber (enclosing 6 $cm^2$ of leaf area) and a $CO_2$ injection system (model 6400-01, LI-COR Inc., Lincoln, NE, USA) for the control of $CO_2$. The light intensity for all measurements was 400 $\mu$mol $m^{-2}.s^{-1}$, provided by a red-blue light source (model 6400-02, LI-COR Inc., Lincoln, NE, USA). The temperature was set at 25 °C while the humidity was set at 60 %. Photosynthetic readings were taken at 0, 50, 100, 200, 400, 600, 800, 1000, 1200, 1400, 1600, 1800, and 2000 $\mu$mol photons $m^{-2}.s^{-1}$ PAR irradiance intervals. Measurements were performed between 09h00 and 15h00 (Thuynsma et al., 2016) on 3 replicates in each treatment for at least 1 h to complete each response curve. All photosynthetic values were adjusted and expressed on a leaf dry mass basis. The light saturation rate of photosynthesis ($P_{max}$), quantum yield ($\varphi$), light compensation point (LCP) and dark respiration were derived from the light–response curves. In contrast, photosynthetic water-use efficiency (WUE) was calculated from measurements of $P_{max}$ and transpiration rate. Pigments associated with photosynthesis were extracted from frozen plant material, assayed in 80 % (v/v) acetone and determined and calculated as previously described (Arnon 1949). The analysis of variance (ANOVA) for the physiological photosynthesis-related parameters was analysed using STATISTICA Version 12 (StatSoft Inc.) to infer differences between treatments at the 95 % confidence level.

### 2.2. Protein extraction and quantification

#### 2.2.1. Protein extraction and digestion

Protein was extracted from *A. thaliana* leaf tissue (100 mg) liquid nitrogen grounded tissue by solubilising tissues in 6 M urea/50 mM Tris–HCl (pH 8.0) protein extraction buffer. The solubilised samples were sonicated for 10 min, followed by centrifugation at 15,000 g for 5 min. The total soluble protein content was determined using a Bio-Rad Protein Assay Kit (I5000001) by measuring the absorbance of the dilution spectrophotometrically at 595 nm, using bovine gamma globulin as a standard (Bradford, 1976).

Next, 50 $\mu$g of protein from each sample was subjected to protein disulfide bridge reduction in 5 mM dithiothreitol (DTT) for 30 min at 37 °C. Subsequently, the cysteine residues were alkylated in 15 mM iodoacetamide (IAA) in the dark for 30 min (Olsen et al., 2004),

followed by predigestion for 4 h at 37 °C with endoproteinase (Trypsin/Lys-C Mix, Mass Spectrometry grade, Promega). Samples were then diluted 6-fold with 50 mM Tris−HCl (pH 8.0) and digested overnight at 37 °C with Trypsin/Lys-C Mix. To terminate the reaction after an overnight digestion, samples were acidified (pH3 or less) by adding trifluoroacetic acid (TFA) to a final concentration of 0.2 % (v/v) (Stefan et al., 2022). The samples were centrifuged at 13 000 x*g* for 10 min to remove particulate materials and immediately desalted using Millipore ZipTipc18 micropipette tips (Millipore, Dublin, Ireland) following the manufacturer's protocol.

#### 2.2.2. Peptide analysis by LC−MS/MS

Tryptic peptide mixtures were analysed by LC/MS/MS using a Nanoflow Easy-nLC1000 (Thermo Scientific) as an HPLC system and a Quadrupole-Orbitrap hybrid mass spectrometer (Q Exactive Plus, Thermo Scientific) as a mass analyser. The 75 $\mu$m × 50 cm analytical column (Thermo Scientific) eluted peptides on a linear gradient running from 4 % to 64 % (v/v) acetonitrile for 240 min and sprayed directly onto a Q Exactive mass spectrometer. MS/MS was used to identify proteins following information-dependent acquisition of fragmentation spectra of multiple charged peptides. Twelve data-dependent MS/MS spectra were acquired for each full-scan spectrum at 60,000 full-width half-maximum resolution. Fragment spectra were acquired at a resolution of 35,000 with an overall cycle time of approximately one second. The mass spectrometry proteomics data was deposited to the ProteomeXchange Consortium via the PRIDE partner repository with the dataset identifier PXD014006.

MaxQuant version 1.4.0.1 was used for protein identification and ion intensity quantitation (Cox and Mann, 2008). The spectra were matched against the *A. thaliana* proteome (TAIR10, 35,386 entries, last accessed February 2024) using Andromeda (Cox and Mann, 2011). The carbamidomethylation of cysteine was set as a fixed modification; methionine oxidations were set as variable modifications. The mass tolerance for the database search was set to 20 ppm for full scans and 0.5 Da fragment ions, and the multiplicity was set to 1. For label-free quantitation, retention time matching between runs was chosen within a time window of 2 min. The peptide false discovery rate (FDR) and protein FDR were set to 0.01, while the site FDR was set to 0.05. Hits to contaminants (e.g., keratins) and reverse hits identified by MaxQuant were excluded from further analysis (Benjamini and Hochberg, 1995).

#### 2.2.3. Proteomic quantitative data analysis

Reported ion intensity values were used for quantitative data analysis. cRacker (Zauber and Schulze, 2012) was used for label-free data analysis of summed peptide ion intensities per protein based on the MaxQuant output (evidence.txt). All proteotypic peptides were used for quantitation. Within each sample, the ion intensities of each peptide ion species (each *m/z*) were normalised against the total ion intensities in that sample (peptide ion intensity/total sum of ion intensities). Subsequently, each peptide ion species (i.e., each *m/z* value) was scaled against the average normalised intensities of that ion across all treatments. Values from three biological replicates were averaged for each peptide after normalisation and scaling. Comparisons between lumichrome-treated plants and controls are displayed as $\log_2$ values and were evaluated using pairwise *t*-tests based on three biological replicates. Multiple false-discovery-rate (FDR) testing corrections were applied according to Benjamini-Hochberg (Benjamini and Hochberg, 1995). Responsive proteins were defined based on a $p\text{-value} < 0.05$ after correcting for multiple tests. The ratios were normally distributed (Supplementary Fig. S1). The data are available via ProteomeXchange with the identifier PXD014006.

### 2.3. Metabolite extraction, derivatisation and determination using GC–TOF–MS

Primary metabolites (50 mg) were extracted from leaf tissues. (Heise et al., 2014; Naake et al., 2024). Metabolites were extracted in a pre-cooled (−20 °C) 80 % [v/v] methanol (Sigma-Aldrich) and ribitol as internal standard. The homogenised samples were shaken for 5 min and centrifuged at 16,000 x*g* for 10 min at room temperature. The supernatant was centrifuged at 16,000 x*g* for 10 min at room temperature, while 200 $\mu$L of the supernatant was transferred to a new tube, freeze-dried by speed-vac for 3 h. Afterwards, the sample tubes were filled with argon, and stored at −80 °C.

Samples were prepared for analysis by resuspending them in 80 % [v/v] methanol and transferring the resuspended samples into sample vials. To render primary metabolites volatile enough for analysis, samples were derivatised according to Lisec et al. (2006). Derivatisation was performed at 37 °C with 20 mg mL$^{-1}$ methoxyamine hydrochloride in pyridine to prevent the formation of multiple derivatives during silylation and agitated for 120 min. This was followed by adding the silylating agent N-Methyl-N-trimethylsilyltrifluoroacetamide (MSTFA) and incubation with shaking at 37 °C for 30 min. An autosampler Gerstel Multi-Purpose system (Gerstel GmbH & Co.KG, Mülheim an der Ruhr, Germany) was used to inject the samples into a gas chromatograph coupled to a time-of-flight mass spectrometer (GC−MS) (Leco Pegasus HT TOF−MS; LECO Corporation, St. Joseph, MI, USA), fitted with a 30 m DB-35 column. Carrier gas was helium at a constant flow rate of 2 ml s$^{-1}$. Injection temperature was 230 °C and the transfer line and ion source were set on 250 °C. Oven temperature was set initially on 85 °C and increased with 15 °C min$^{-1}$ to 360 °C. The mass spectra were recorded at 20 scans s$^{-1}$ with *m/z* 70−600 scanning range. Mass chromatograms were assessed with Chroma TOF 4.5 (Leco) and TagFinder 4.2 software (Luedemann et al., 2012). Metabolites were identified by comparing their mass spectra and retention indices with those of standards. At the same time, peak areas in each chromatogram were adjusted to both ribitol internal standards and the respective exact sample weight. In addition the Golm Metabolome database was used for cross-referencing of the mass spectra (Harb et al., 2015).

## 3. Results

### 3.1. Lumichrome enhances various facets of photosynthesis

Analysis of 5-week-old *A. thaliana* rosette leaves revealed an increase in the maximum photosynthetic rate ($P_{max}$; Fig. 1A), stomatal conductance ($g_s$; Fig. 1B) and transpiration rate (*E*; Fig. 1C) increased following lumichrome treatment, alongside a decrease in water use efficiency (*WUE*; Fig. 1D). However, the efficiency of light utilization during photosynthetic $CO_2$ fixation in terms of quantum yield ($\varphi$), was not significantly affected (Fig. 1E). With regards to the photosynthetic pigments, concentrations of chlorophyll ***a*** and chlorophyll ***b*** were significantly increased following lumichrome treatment (Fig. 1F), whereas the carotenoid levels were unaltered (Fig. 1G).

### 3.2. Differential protein profiles in response to lumichrome

A total of 1738 proteins were identified, from which *t*-test analysis revealed 284 proteins that exhibited significant differences in quantity. However, correction for multiple testing using the Benjamini−Hochbeg analysis showed only 46 proteins that were significantly different between treatment and controls. Among these 46 proteins, 22 were upregulated, while 24 were downregulated (Table S1). Analysis of functional categories showed that 20 % of the identified proteins were involved in the RNA and protein metabolism and stress response, respectively. In comparison, 15 % were involved in photosynthesis (Fig. 2A). Regarding the overexpression response, the most

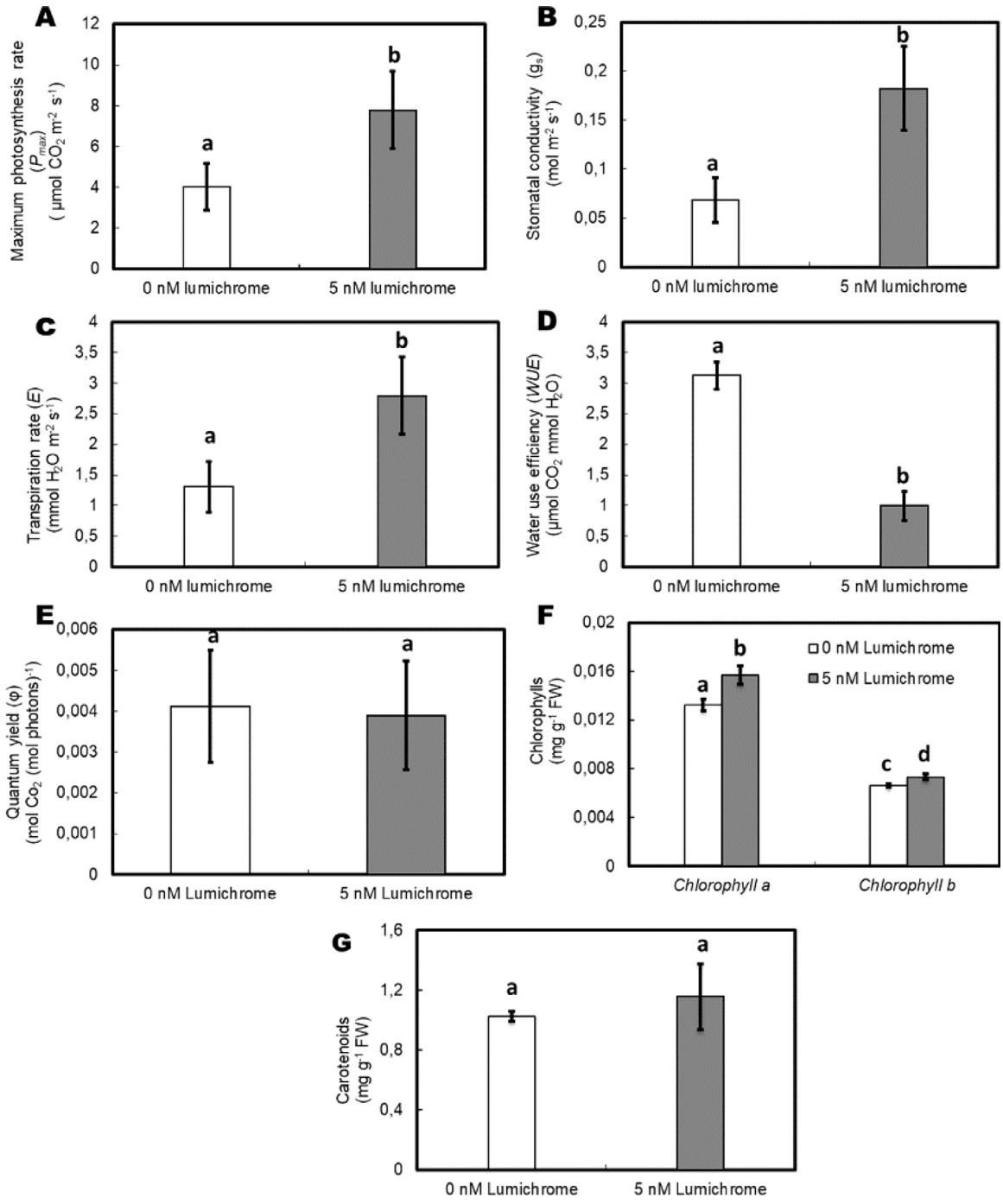


**Fig. 1.** Photosynthetic parameters and pigments in *A. thaliana* in response to 5 nM lumichrome treatment. Net photosynthesis rate ($P_n$) (Fig. 1A), stomatal conductance to water vapour ($g_s$) (Fig. 2B), transpiration rates (*E*) (Fig. 1C), intrinsic water use efficiency (WUE) (D), photon yield (E), chlorophyll pigments (F) and carotenoids (G) in 5-week-old *A. thaliana* leaves. The error bars denote the standard errors of the means ($n = 6$). Within the graphs, treatments marked with the same letters were not significantly different from one another ($p < 0.05$; Games–Howell *post hoc* test).

widely upregulated represented categories were 27 % for stress response and 23 % for photosynthesis, while protein metabolism and redox homeostasis had 18 % respectively. Other functional categories of upregulated protein include 9 % for carbon metabolism and 5 % for hormone metabolism (Fig. 2B). A similar response trend was demonstrated for the downregulated proteins, with the most significant number of proteins also being associated with protein metabolism (21 %) and stress response (17 %). Other downregulated functional categories included amino acid, transport and carbon metabolism (Fig. 2C).

### 3.2.1. Changes in photosynthesis- and carbon metabolism-related proteins

According to the MapMan metabolism overview (Fig. 3), lumichrome application to *A. thaliana* altered the photosynthesis light reaction by inducing a high abundance of the oxygen-evolving protein 2 (OEE2), such as the PHOTOSYSTEM II SUBUNIT Q1 (PSBQ-1; At4g21280) and the PHOTOSYSTEM II SUBUNIT Q2 (PSBQ-2 (At4g05180). In addition, our results revealed significantly increased levels of ATP SYNTHASE DELTA SUBUNIT (ATPD; At4g09650), which is a chloroplast ATPase synthase protein that forms the catalytic

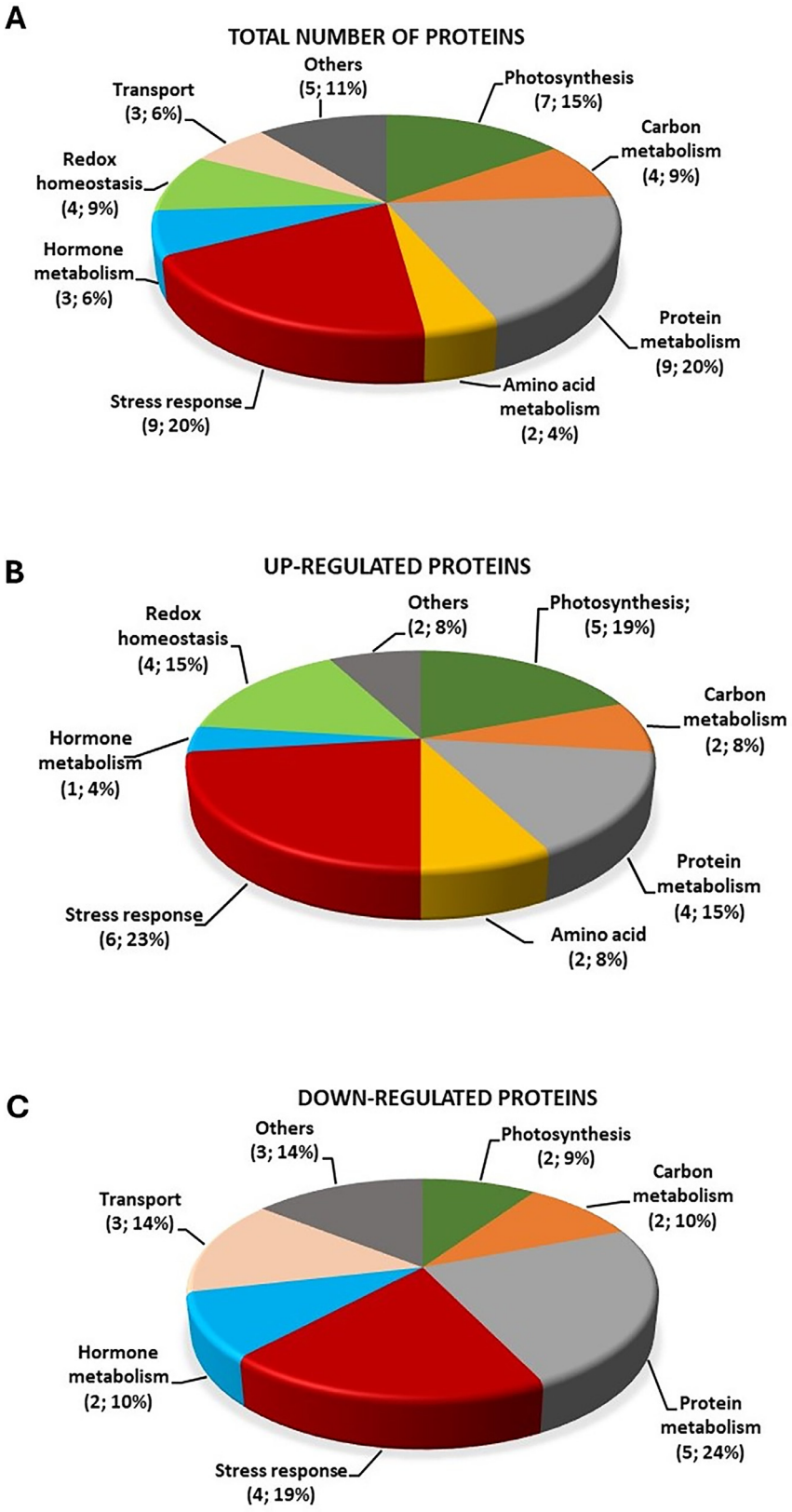


**Fig. 2.** Functional classification of differential protein profiles in lumichrome treated *A. thaliana*. The fuctional categories (Fig. 2A and the expression trend for the respective functional categories (Fig. 2B; C) were identified with Mapman. The percentage of each functional group was obtained based on the calculated absolute number of proteins under each functional group subtracted from the total number of significantly differentially expressed proteins.

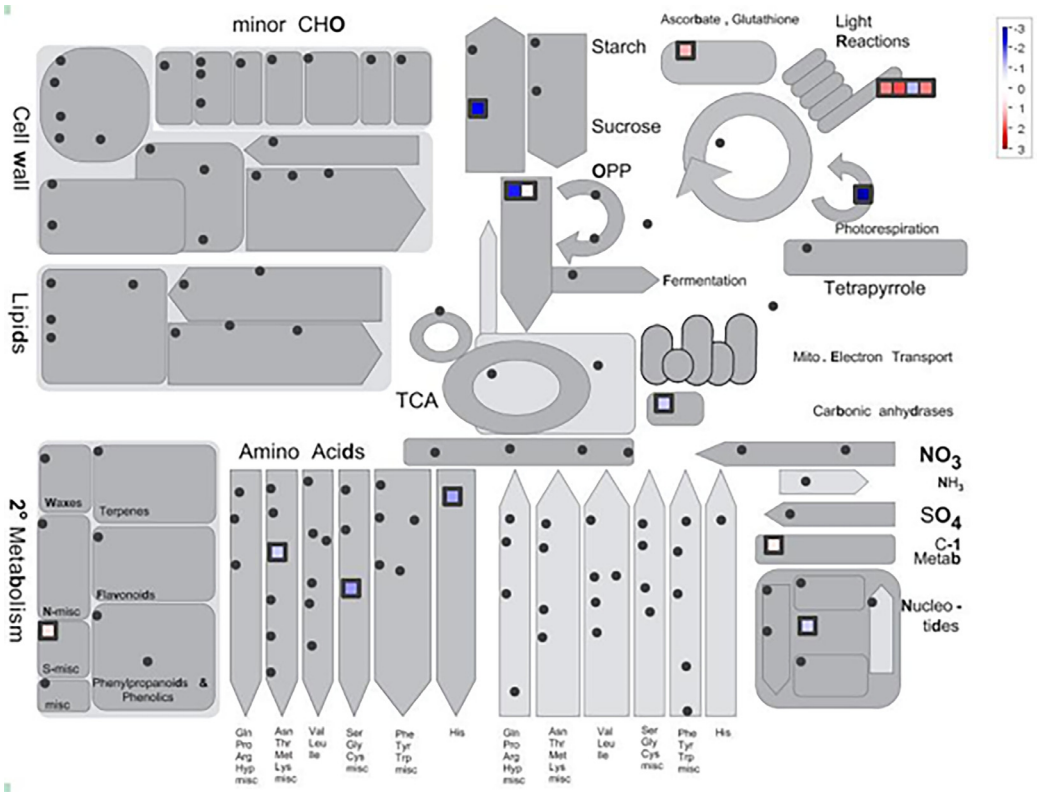


**Fig. 3.** MapMan general overview of a pairwise comparison of lumichrome-treated *A. thaliana* rosette leaves relative to the untreated control. Proteins that were shown to be differentially expressed using $p < 0.05$ as a cutoff value were imported. Red represents proteins that were upregulated, while blue indicates those that were downregulated upon 5 nM lumichrome treatment. The magnitude of the protein profiles is indicated by the colour intensity.

entity in the chloroplast ATP synthase electron transport chain. THE PHOTOSYSTEM I REACTION CENTRE SUBUNIT E1 (PSAE-1; At4g28750) protein was significantly repressed, while thylakoid lumenal protein, namely the Maintenance of Photosystem II under HIGH LIGHT 2 C-TERMINAL DOMAIN-CONTAINING PROTEIN (MPH2; At4g02530) was significantly increased following lumichrome treatment (Fig. 3). Furthermore, proteins involved in the light and circadian rhythm signalling proteins, such as TRANSLOCON AT THE INNER ENVELOPE MEMBRANE OF CHLOROPLASTS 62 (TIC62; At3g18890) and the PLASTID TRANSCRIPTIONALLY ACTIVE 16 (PTAC16; At3g46780) were significantly suppressed and increased respectively (Table 1).

Treating *Arabidopsis* with lumichrome also affected the protein levels involved in carbon metabolism. The proteins associated with partitioning carbohydrates between starch and sucrose were significantly altered (Table 1). This included an increase in the glycolytic dually targeted FRUCTOSE BISPHOSPHATE ALDOLASE (FBA8; At3g52930) and the suppression of the plastid PHOSPHOGLUCOMUTASE 1 (PGM1; At5g51820). In addition, the One-carbon (1C) metabolism protein TRANSHYDROXYMETHYLTRANSFERASE 1 (SHMT1; At4g37930) was upregulated following lumichrome treatment (Table 1).

### 3.2.2. Changes in the RNA and protein metabolism and amino acids-related proteins

Lumichrome application on *A. thaliana* induced protein changes involved RNA processing, synthesis, initiation, targeting, posttranslational modification, protein degradation and folding. REACTIVE INTERMEDIATE DEAMINASE A (RIDA; At3g20390), a protein associated with RNA processing ribonuclease was increased. Despite the repressed levels of RIBOSOMAL PROTEIN L14 (RPL14; Atcg00780), there was an overexpression of ribosomal synthesis associated proteins such as RIBOSOMAL PROTEIN L12-C (RPL12-C; At3g27850). Protein synthesis initiation and protein targeting associate proteins may both have been inhibited, as revealed by the decreased levels of the EUKARYOTIC INITIATION FACTOR 4B2 (EIF4B2; At1g13020 and the chloroplast TRANSLOCON AT THE OUTER ENVELOPE MEMBRANE OF CHLOROPLASTS 159 (TOC159; At4g02510) respectively. Post-translational modification proteins HISTIDINE TRIAD NUCLEOTIDE-BINDING 2 (HINT2; At1g31160) and the co-chaperone SUPPRESSOR OF THE G2 ALLELE OF SKP1 A (SGT1A; At4g23570) showed differing responses to lumichrome, with HINT2 being upregulated and SGT1A being downregulated. The serine protease degradation proteins, including CARBOXYL-TERMINAL PROCESSING (CTPA; At4g17740) and DEG PROTEASE 8 (DEG8) proteases, were inhibited, whereas PROTEASOME REGULATOR1 (PTRE1; At3G53970), the proteasome related to ubiquitin protein degradation, was upregulated. The CHAPERONIN 20 (CPN20; At5g20720), a protein involved in protein folding, was also increased following lumichrome applications (Table 1; Fig. 4).

Lumichrome applications induced the downregulation of the three identified proteins associated with serine-glycine-cysteine, histidine bifunctional and the aspartate-methionine biosynthesis groups, respectively. These include proteins such as the O-ACETYL SERINE (THIOL) LYASE B (OASTLB; At2g43750), HISTIDINE BIOSYNTHESIS BIFUNCTIONAL PROTEIN (HISN2; At1g31860) and the METHIONINE ADENOSYLTRANSFERASE 3 (MAT3; At2g36880)

### 3.2.3. Stress response-related proteins

Treating *A. thaliana* with lumichrome resulted in a high representation of stress-related proteins. Amongst the abiotic stress-related proteins, the chloroplast HEAT SHOCK PROTEIN 70-1 (cPHSC70-1; At4g24280) were significantly increased. However, the DEHYDRIN FAMILY PROTEIN (ERD14; At1g76180), METHIONINE

**Table 1**
Protein profiling of *A. thaliana* rosette leaves in response to 5 nM lumichrome treatment.

| AGI | Protein name | Biological function | log2 fold change ratio 5/0 | $P < 0.05$ BH.corrected |
|---|---|---|---|---|
| **Photosynthesis** | | | | |
| At4g21280 | PHOTOSYSTEM II SUBUNIT QA (PSBPQ-1) | Photosystem II light reaction | 1.68 | 0.002 |
| At4g05180 | PHOTOSYSTEM II SUBUNIT Q-2 (PSBQ-2) | Photosystem II light reaction | 2.02 | 0.005 |
| At4g09650 | ATP SYNTHASE DELTA-SUBUNIT (ATPD) | ATP synthase electron transport chain | 1.69 | 0.001 |
| At4g28750 | PHOTOSYSTEM I REACTION CENTRE SUBUNIT 1(PSAE-1) | Photosystem I light reaction | −1.24 | 0.000 |
| At3g14415 | GLYCOLATE OXIDASE 2 (GOX2) | Photorespiration | −4.11 | 0.049 |
| At4g02530 | MAINTENANCE OF PHOTOSYSTEM II UNDER HIGH LIGHT 2 (MPH2) | PSII protection | 1.16 | 0.026 |
| At3g46780 | PLASTID TRANSCRIPTIONALLY ACTIVE 16 (PTAC16) | Circadian rhythm | 0.45 | 0.041 |
| **Carbon metabolism** | | | | |
| At1g43670 | CYTOSOLIC FRUCTOSE-1,6-BISPHOSPHATASE (FBPASE) | Major CHO metabolism-sucrose synthesis | −2.45 | 0.001 |
| At5g51820 | PHOSPHOGLUCOMUTASE 1 (PGM1) | Glycolysis | −2.28 | 0.032 |
| At3g52930 | FRUCTOSE-BISPHOSPHATE ALDOLASE 8 (FBA8) | Glycolysis | 0.49 | 0.031 |
| At5g14740 | CARBONIC ANHYDRASES (CA2) | Glycolysis<br>TCA / organisational transformation | −1.09 | 0.016 |
| **C1-metabolism** | | | | |
| At4g37930 | SERINE TRANSHYDROXYMETHYLTRANSFERASE 1 (SHMT1) | C1: glycine hydroxymethyltransferase | 0.62 | 0.033 |
| **RNA processing and protein metabolism** | | | | |
| At3g20390 | REACTIVE INTERMEDIATE DEAMINASE A (RIDA) | RNA processing-ribonucleases | 0.93 | 0.025 |
| At3g27850 | RIBOSOMAL PROTEIN L12-C (RPL12-C) | Protein synthesis-ribosomal protein | 2.33 | 0.026 |
| Atcg00780 | RIBOSOMAL PROTEIN L14 (RPL14) | Protein synthesis-ribosomal protein | −1.65 | 0.017 |
| At1g13020 | EUKARYOTIC INITIATION FACTOR 4B2 (EIF4B2) | Protein synthesis initiation | −0.90 | 0.002 |
| At4g02510 | TRANSLOCON AT THE OUTER ENVELOPE MEMBRANE OF CHLOROPLASTS 159 (TOC159) | Chloroplast protein targeting | −3.00 | 0.002 |
| At3g18890 | TRANSLOCON AT THE INNER ENVELOPE MEMBRANE OF CHLOROPLASTS 62 (TIC62) | Protein importation | −1.44 | 0.012 |
| At1g31160 | HISTIDINE TRIAD NUCLEOTIDE-BINDING 2 (HINT2) | Protein posttranslational modification | 1.00 | 0.008 |
| At4g23570 | SUPPRESSOR OF THE G2 ALLELE OF SKP1 A (SGT1A) | Protein posttranslational modification | −1.41 | 0.047 |
| At4g17740 | CARBOXYL-TERMINAL PROCESSING A (CTPA) | Protein degradation-serine protease | −0.81 | 0.018 |
| At5g39830 | DEG PROTEASE 8 (DEG8) | Protein degradation-serine protease | −1.58 | 0.017 |
| At3g53970 | PROTEASOME REGULATOR1 (PTRE1) | Protein degradation-ubiquitin, proteasome | 0.88 | 0.035 |
| At5g20720 | CHAPERONIN 20 (CPN20) | Protein folding | 0.55 | 0.034 |
| **Amino acid metabolism** | | | | |
| At2g43750 | O-ACETYLSERINE (THIOL) LYASE B (OASTLB) | Synthesis: Serine-glycine-cysteine group | −1.52 | 0.015 |
| At1g31860 | HISTIDINE BIOSYNTHESIS BIFUNCTIONAL PROTEIN (HISN2) | Synthesis: Histidine bifunctional | −1.46 | 0.007 |
| At2g36880 | METHIONINE ADENOSYLTRANSFERASE 3 (MAT3) | Synthesis: Aspartate-methionine | −1.08 | 0.003 |
| At5g26000 | THIOGLUCOSIDE GLUCOHYDROLASE 1 (TGG1) | myrosinases-lectin-jacalin | 0.75 | 0.045 |
| **Nucleotide metabolism** | | | | |
| At4g11010 | Nucleoside diphosphate kinase 3 (NDPK3) | Phosphotransfer and pyrophosphatase nucleotides | −1.01 | 0.013 |
| **Metal Handling** | | | | |
| At4g14710 | ACIREDUCTONE DIOXYGENASE [IRON (II)-REQUIRING]/ METAL ION BINDING (ATARD2) | Regulation | 0.85 | 0.033 |
| **Transport** | | | | |
| At1g22530 | PATELLIN 2 (PATL2) | Transport-misc | −0.89 | 0.009 |
| **Stress response** | | | | |
| At4g24280 | CHLOROPLAST HEAT SHOCK PROTEIN 70-1 (cPHSC70-1) | Abiotic heat stress | 0.54 | 0.003 |
| At4g23670 | MAJOR LATEX PROTEIN 6 (MLP6) | Abiotic | 0.95 | 0.043 |
| At1g76180 | DEHYDRIN FAMILY PROTEIN (ERD14) | Abiotic stress | −0.70 | 0.032 |
| At3g07230 | WOUND-RESPONSIVE PROTEIN-RELATED | Abiotic touch/wounding | 0.79 | 0.048 |
| At5g03660 | N-ACETYL TRANSFERASE 60 (NAA60) | biotic salt stress | −0.69 | 0.023 |
| **Redox homeostasis** | | | | |
| At1g03680 | THIOREDOXIN M-TYPE 1 (TRX-M1) | Thioredoxin | 0.72 | 0.004 |
| At3g15360 | THIOREDOXIN M-TYPE 4 (TRX-M4) | Thioredoxin | 0.74 | 0.011 |
| At1g07890 | ASCORBATE PEROXIDASE 1 (APX1) | Ascorbate and glutathione redox | 1.31 | 0.011 |
| At3g52960 | PLASTID PEROXIREDOXIN-II-E (PRX-IIE) | Peroxiredoxin redox | 1.00 | 0.004 |
| **Hormone signalling** | | | | |
| At3g02480 | ABSCISIC RESPONSE PROTEIN (LEA-ABR) | abscisic acid induced-regulated | 2.65 | 0.036 |
| At3g25770 | ALLENE OXIDE CYCLASE 2 (AOC2) | Jasmonate synthesis | −0.68 | 0.006 |

(*continued*)

**Table 1** (*Continued*)

| AGI | Protein name | Biological function | log2 fold change ratio 5/0 | *P* < 0.05 BH.corrected |
|---|---|---|---|---|
| **Miscellaneous/Unknown** | | | | |
| At3g05900 | NEUROFILAMENT PROTEIN-RELATED | Unknown | 0.51 | 0.000 |
| At1g21680 | DPP6 N-TERMINAL DOMAIN-LIKE PROTEIN | Unknown | −0.71 | 0.019 |
| At5g49110 | FANCONI ANEMIA GROUP I-LIKE PROTEIN | Unknown | −2.47 | 0.015 |
| At2g23120 | LATE EMBRYOGENESIS ABUNDANT PROTEIN, GROUP 6 | Unknown | 1.00 | 0.008 |

Values are represented as log2-fold changes of protein profiles of lumichrome-treated compared to the untreated control and the *p*-value adjusted (adj. value) to correct for the probability of false positives using the FDR correction (Benjamini and Hochberg, 1995). *p-value* < 0.05 was deemed significant.

ADENOSYLTRANSFERASE 3 (MAT3; At2g36880) and N-ACETYL TRANSFERASE 60 (NAA60; At5g03660) were significantly repressed in lumichrome treated plants relative to their control. On the other hand, there was general repression of biotic stress-related proteins, including MAJOR LATEX PROTEIN 6 (MLP6; At4g23670), Wound-responsive protein-related (At3g07230), THIOGLUCOSIDE GLUCOHYDROLASE 1 (TGG1; At5g26000) and RMLC-LIKE CUPINS SUPERFAMILY PROTEIN (ATARD2; At4g14710).

### 3.2.4. Hormone signaling, redox homeostasis regulation, and other proteins identified in response to lumichrome application

The results demonstrated an altered abscisic acid hormone metabolism through the highly increased levels of the Late embryogenesis abundant ABSCISIC RESPONSE PROTEIN (ABR; At3g02480). Conversely, expression of ALLENE OXIDE CYCLASE 2 (AOC2; At3g25770), the protein involved in the jasmonate hormone signalling, was altered (Table 1). Lumichrome treatment significantly induced the abundance of several proteins, which are essential for scavenging reactive oxygen species in the light regulation of photosynthetic metabolism (Table 1). This group included highly abundant reactive oxygen species (ROS) redox signalling-related proteins such as THIOREDOXIN M-TYPE 1 (TRX-M1; At1g03680) and THIOREDOXIN M-TYPE 4 (TRX-M4; At3g15360). In addition, the redox changes associated with the ascorbate–glutathione redox regulation protein ASCORBATE PEROXIDASE 1 (APX1; At1g07890) and the peroxiredoxin redox regulation was altered via a significant increase in the plastid PEROXIREDOXIN-II-E (PRX-IIE; At3g52960). (Table 1; Fig. S2).

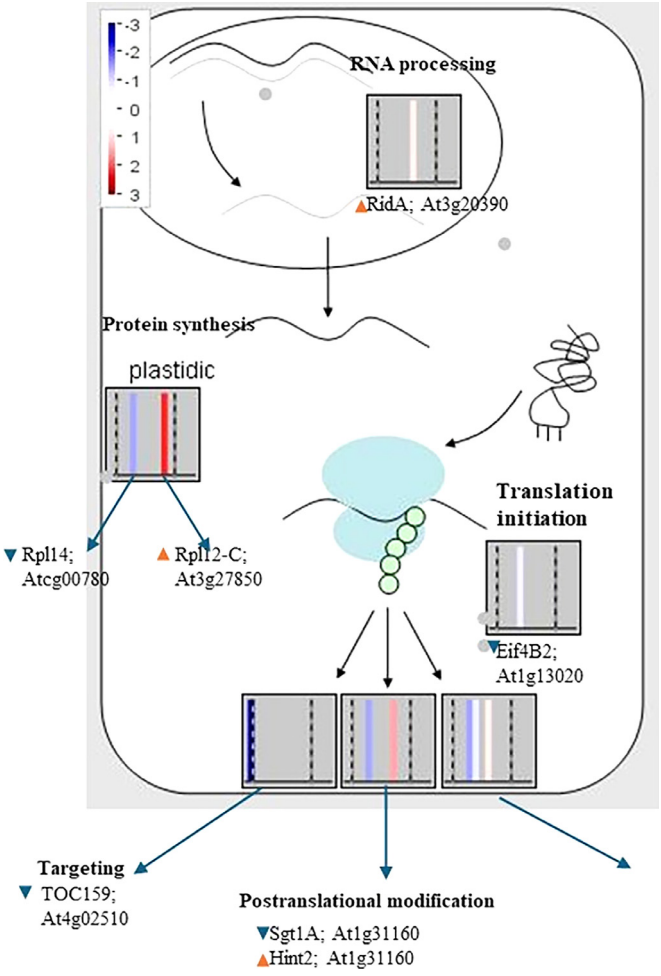


**Fig. 4.** Overview of a MapMan RNA–protein synthesis, posttranslational modification and degradation in *A. thaliana* treated with lumichrome. Red and blue histograms denote upregulated and downregulated proteins, respectively.

Lumichrome treatment downregulated proteins involved in transport. This includes the induced inhibition of the TRANSLOCON AT THE INNER ENVELOPE MEMBRANE OF CHLOROPLASTS 62 (TIC62; At3g18890) and the PATELLIN 2 (PATL2; At1g22530). Moreover, the results revealed an induced repression of the phosphotransfer and pyrophosphatase nucleotide-related protein called NUCLEOSIDE DIPHOSPHATE KINASE 3 (NDPK3). In terms of metal handing metabolism, lumichrome treatment induced the abundance of the regulatory ACIREDUCTONE DIOXYGENASE [IRON (II)-REQUIRING]/ METAL ION BINDING (ATARD2; At4g14710), while the metal binding, chelation and storage were negatively altered through the decreased levels of the METHIONINE ADENOSYLTRANSFERASE 3 (MAT3; At2g36880).

### 3.3. Changes in the metabolite profile in response to lumichrome

GC–TOF–MS metabolite profile analysis revealed 60 metabolites (Table S2), of which 15 were significantly affected following lumichrome treatment. This analysis indicated an accumulation of soluble sugars and alcohols, including fructose, glucose, maltose, sucrose, trehalose and rhamnose. Amongst these, fructose and glucose showed the most significant increases compared with those in the control plants. In addition, treatment with lumichrome led to the accumulation of various amino acids, with proline showing the highest accumulation, followed by glycine (Table 2).

## 4. Discussion

### 4.1. Photosynthetic changes in response to lumichrome treatment

With the present study, we shed more light on the possible effect of lumichrome on the photosynthesis efficiency and the ultimate growth of *A. thaliana*. In concert with previous studies on several plant species (Gouws et al., 2012; Khan et al., 2008; Phillips et al., 1999; Volpin and Phillips, 1998), treating *A. thaliana* with lumichrome induced an increase in photosynthesis rate. The enhanced photosynthesis rate was accompanied by increased stomatal conductivity and transpiration rate, whereas the water use efficiency was inhibited. According to Leakey et al. (2009) and Sreeharsha et al. (2015), the reduction in stomatal aperture under elevated $CO_2$ has

**Table 2**
Changes in the sugar abundance of *A. thaliana* rosette leaves in response to 5 nM lumichrome treatment.

| Metabolite | Fold2 change ratio | *t*-test ($p \leq 0.05$) |
|---|---|---|
| Fructose | 1.151 | 0.006 |
| Glucose | 1.128 | 0.036 |
| Sucrose | 0.225 | 0.019 |
| Maltose | 0.706 | 0.033 |
| Trehalose, alpha- alpha | 0.596 | 0.010 |
| Rhamnose | 0.305 | 0.016 |
| Asparagine | 0.597 | 0.021 |
| Glycine | 1.440 | 0.022 |
| Phenylalanine | 0.525 | 0.026 |
| Proline | 1.457 | 0.036 |
| Putrescine | 0.544 | 0.006 |
| Tyrosine | 0.495 | 0.034 |
| Valine | 0.379 | 0.037 |
| Glutamic acid | 0.275 | 0.014 |
| Sorbitol | 0.505 | 0.035 |

GC–MS analyses of *A. thaliana* rosette leaf metabolites in response to lumichrome. The values are expressed as the fold change ratio of the treated group to the untreated control group. Response ratio = intensity of the mass of the specific metabolite normalised to fresh weight and the internal standard ribitol. Significant changes were evaluated using a *t-test* ($p \leq 0.05$).

been associated with increased intrinsic water use efficiency with potential benefits for plant growth (Leakey et al., 2009; Sreeharsha et al., 2015).

On the contrary, reductions in stomatal aperture can negatively impact photosynthesis because of diffusional constraints and increased leaf temperature (Matthews and Lawson, 2018). In the current study, an increased stomal conductivity and transpiration rate may have enhanced the $CO_2$ uptake, subsequently increasing the photosynthesis rate (Kusumi et al., 2012). However, the correlations between high photosynthesis rate and low water use efficiency following lumichrome treatment must be clarified. In addition, the increase in chlorophyll *a* and *b* suggested an enhanced capturing and absorption of solar energy, which might have promoted the transition of electrons to the photosynthetic reaction centre (Fromme et al., 2003).

Besides the physiological regulation, the molecular regulation of the photosynthetic capacity and efficiency depends on the highly flexible regulation of the catalytic four major protein complexes, including photosystem I (PSI), photosystem II (PSII), cytochrome b6f and ATPase (Munekage et al., 2002; Tikkanen and Aro, 2014). In that respect, a triggered increase in PHOTOSYSTEM II SUBUNIT Q1 (PSBQ-1) and PHOTOSYSTEM II SUBUNIT Q2 (PSBQ-2) extrinsic subunits of the photosystem II (PS II) was observed in lumichrome treated plants compared to the control. Previous reports indicated that cyanobacterial mutants lacking PSBP and PSBQ proteins exhibit significant defects in PSII function. These include lower oxygen-evolving activity, reduced quantum yield, a slower electron transfer rate at the donor side of PSII, and diminished photoautotrophic growth. (Chaiwongsar et al., 2012). In another study on spinach, it was revealed that the N-terminal of PSBP is necessary for oxygen evolution and induces the protein conformation required for the retention of $Ca^{2+}$ and $C^{-1}$ needed for PSII activity. Loss of PSBP function can cause defects in the conformational changes in the Mn cluster of the water oxidation machinery. However, PSBQ can compensate for the N-terminal functional defect of PSBP, indicating that PSBQ helps to stabilise PSBP in PSII (Ifuku et al., 2005; Kakiuchi et al., 2012). Therefore, the upregulated PSBQ-1 and PSBQ-2 could have collectively played a role in enhancing the conformational Mn cluster of the water oxidation machinery and stabilising PSII.

The protection of PSII from photodamage was likely due to the high abundance of the MAINTENANCE OF PHOTOSYSTEM II UNDER HIGH LIGHT 2 (MPH2) protein, which enhances photosynthetic efficiency and productivity. An *A. thaliana* MPH2 null mutant has revealed a deficiency in disassembling and repairing damaged monomeric complexes. This deficiency led to reduced PSII efficiency, indicating that the MPH2 protein is crucial for maintaining proper photosynthetic function, especially under changing light conditions. Additionally, the mutant plants exhibited a significantly reduced growth rate phenotype when exposed to photo-inhibitory and fluctuating light conditions (Liu and Last, 2017).

Lumichrome treatment further increased the expression of the chloroplast ATP SYNTHASE DELTA SUBUNIT (ATPD) protein. Repression of cpATPase synthase has previously demonstrated a strongly inhibited linear electron flux due to decreased rates of plastoquinol reoxidation at the cytochrome b6f complex. This mutation also triggered nonphotochemical quenching at very low light intensities, thereby strongly reducing the quantum efficiency of $CO_2$ fixation. This resulted in impaired photosynthetic electron transport, $CO_2$ assimilation, and plant growth due to the consequential over-acidification of the thylakoid lumen (Kanazawa and Kramer, 2002; Rott et al., 2011; Rühle and Leister, 2015). Conversely, overexpressing the ATPD subunit of the chloroplast ATP synthase in rice increased the abundance of the whole ATPase complex, including increased ATP synthase activity, resulting in higher electron transport rates and high irradiance, as well as higher assimilation rates (Ermakova et al., 2022). The increase in ATPD and the stable quantum yield following lumichrome treatment could have been attributed to higher linear electron transport, carbon assimilation and photosynthesis efficiency.

On the other hand, the PHOTOSYSTEM I REACTION CENTRE SUBUNIT 1 (PSAE-1) was suppressed following lumchrome treatment. PSAE is part of the extrinsic protein subunits that form the docking site of ferredoxin at the acceptor side of PSI (Caspy and Nelson, 2018; Kubota-Kawai et al., 2018; Nelson and Yocum, 2006). In *A. thaliana*, disruption of the *PSAE1* gene has been reported to lead to enhanced PSII photoinhibition and lower level of P700 oxidation under steady-state conditions with a consequential stunted growth and light-green pigmentation phenotype (Varotto et al., 2000). Furthermore, *psae1-3* knockout mutant (Ihnatowicz et al., 2007) plants have shown a higher NPQ and a higher efficiency of cyclic electron flow than the wild-type (Hald et al., 2008). Plants treated with lumichrome did not show light green pigmentation, even though the PSAE-1 protein representation was decreased. This may be due to the promotion of effective photosynthesis through efficient cyclic electron transport of PSI and dissipation of excess heat through the NPQ mechanism. Our study indicates that both the linear and cyclic electron pathways, as well as photoprotection mechanisms, contribute to enhancing photosynthesis efficiency.

Interestingly, the PLASTID TRANSCRIPTIONALLY ACTIVE CHROMOSOME 16 (PTAC16), a protein complex attached to the plastid membrane that plays a role in plastid transcription and translation, was over-expressed. Although the function of most TAC genes is not yet known, knockout of the *PTAC14* gene in *A. thaliana* led to the blockage of thylakoid formation in the initial process of chloroplast development and downregulated transcript levels of plastid-encoded polymerase (PEP)-dependent genes were downregulated (Gao et al., 2012). Knockout *ptac* seedlings developed impaired plastid structure with consequentially white or yellow cotyledons and failed to accumulate chlorophyll even under low light intensities (Pfalz et al., 2006), and downregulated levels of plastid-encoded polymerase (PEP) responsible exclusively for the expression of chloroplast-encoded photosynthetic genes (Gao et al., 2012, 2011). The upregulation of PTAC16, coupled with increased chlorophyll *a* and *b* and induced expression of photosynthesis-related genes in the current study, could suggest an optimal plastid structure and plastid metabolism (Inomata et al., 2018).

Central for the ability of chloroplast metabolism to rapidly respond to changes in light intensity is the ability to counteract the

production of singlet oxygen ($^1O_2$) at photosystem (PS) II and superoxide anion ($O_2$) at PSI (Cejudo et al., 2021). We observed that the carotenoid content in lumichrome-treated plants remained unaffected compared to the relative control. This might imply that the steady amount of carotenoid was optimal to deactivate the triple chlorophyll and singlet oxygen efficiently, as well as dissipate excess light energy to prevent photodamage of the photosynthetic apparatus in LHCs of PSII, thus avoiding the oxidative damage of ROS and allowing their signalling activity (Jahns and Holzwarth, 2012; Sun et al., 2022).

Furthermore, there was a high abundance of the THIOREDOXIN M-TYPE 1 (TRX-M1) and the THIOREDOXIN M-TYPE 4 (TRX-M4) proteins, which are essential redox regulators in the light regulation of photosynthetic metabolism through reducing target proteins, thus acting as molecular redox switchers by transferring electrons to a pair of disulphide-bonded cysteines (Collin et al., 2003). A pale-green leaf, disruption of the redox status of intermolecular disulfide bonds in PSII core proteins and the resultant elevated levels of ROS have been reported in *A. thailana* mutant deficient in TRX-M genes (Wang et al., 2013a, 2013b). There was also a high abundance of PLASTID PEROXIREDOXIN-II-E (PRX-IIE), a protein with similar thioredoxin fold structures and a function of maintaining proper ROS homeostasis within plant cells (Dreyer et al., 2021). This further implied the possible peroxidase/thioredoxin (PRXR/TRX) antioxidant defence system, in which TRX coupled with TRX-dependent peroxidase (PRXS) scavenges the excess hydrogen peroxide and peroxides (Kekulandara et al., 2018) thereby improving $CO_2$ assimilation rate and plant growth (Okegawa and Motohashi, 2015). In addition, the cytosolic removal of the $H_2O_2$ removal and regulation of ROS could have been mitigated by the increase in the cytosolic ASCORBATE PEROXIDASE 1 (APX1) (Mauceri et al., 2024).

### 4.2. Lumichrome altered carbon metabolism probably through enhanced sucrose partitioning

A transcriptomic study on tomato and *Lotus* reported that the role of lumichrome in carbon partitioning was associated with enhanced starch accumulation, which was possibly attributed to a rise in plastidial *GLYCERALDEHYDE-3-PHOSPHATE DEHYDROGENASE (GAPDH)* transcripts and NAD-dependent enzyme activity (Gouws et al., 2012). Previously, tomato root proteomic studies revealed that lumichrome treatment reduced levels of GAPC1, also known as plastid-phosphorylated NAD-specific glyceraldehyde-3-phosphate dehydrogenase (Gouws, 2009). Plastidial GAPC, along with phosphoglycerate kinase, is involved in starch breakdown for the production of ATP needed for starch metabolism in green and nongreen plastids, as well as serine metabolism (Backhausen et al., 1998; Muñoz-Bertomeu et al., 2009; Toujani et al., 2013). However, our current proteomic study on *A. thaliana* revealed a decrease in the levels of the plastidial PHOSPHOGLUCOMUTASE 1 (PGM1) protein, an essential protein for the second step of starch biosynthesis (Manjunath et al., 1998), which converts glucose-6-phosphate into glucose-1-phosphate (Müller-Röber et al., 1992). *A. thaliana* mutants in which the activities of PGM1 are reduced or abolished have significantly reduced levels of leaf starch or a starchless phenotype (Caspar et al., 1985; Lin et al., 1988). In addition, lumichrome treatment induced the repression of the cytosolic glycolystic FRUCTOSE-1,6-BISPHOSPHATE 8 (FBA8). Although, cytosolic FBA plays a catalytic role in the reversible conversion of fructose-1,6-bisphosphate (FBPase) to glyceraldehyde-3-phosphate (G3P) and dihydroxyacetone phosphate (DHAP) (Cai et al., 2016; Lu et al., 2012), an increase in the expression of FBA8 was accompanied by a decrease in FRUCTOSE-1,6-BISPHOSPHATE (FBPase) protein. Previous studies reported a positive correlation where on over-expression of the FBA gene in *A. thaliana* increased sucrose synthesis, sugar accumulation, and increased photosynthetic and accelerated plant growth (Cho et al., 2012). On the other hand, the decreased expression of the FBA gene in *A. thaliana* and *Solanum tuberosum* led to a reduced sucrose synthesis, accumulated intermediate metabolites, and eventually blocked photosynthesis (Cho et al., 2012; Zrenner et al., 1996). The increased levels of FBA8 in the current study may have contributed to the increased sucrose synthesis, sugar accumulation and photosynthesis rate. It is therefore proposed that lumichrome modifies carbon partitioning pathways, in which the cytosolic FBA8 underpins the glycolysis and the carbohydrate partitioning in the cytosol, where water soluble carbohydrates provide both an energy source and building blocks for biomass production and maintenance, illustrating biomass production's dependence on carbon fixation in lumichrome-treated plants (Koch, 2004).

### 4.3. Protein metabolism in response to lumichrome treatment

Lumichrome treatment induced an altered RNA processing, ribosomal synthesis, initiation, targeting, post-translational modification, protein degradation and protein folding. This includes an increase in the plastid REACTIVE INTERMEDIATE DEAMINASE A (RIDA), which is involved in damage pre-emption processing by converting an aggressively reactive product into a more benign one, thereby forestalling damage (Lambrecht et al., 2013; Niehaus et al., 2014). Plants lacking RIDA showed defects in plastids (Niehaus et al., 2014), which could further affect the photosynthesis capacity and efficiency. Simultaneously, the expression of RIBOSOMAL PROTEIN L12-C (RPL12-C) was upregulated, while the RIBOSOMAL PROTEIN L14 (RPL14) was underrepresented. This might have suggested that the loss of RPL14 was compensated by the high abundance of RPL12C in enhancing protein synthesis and, consequently, playing an essential role in metabolism, cell division, and growth (Wang et al., 2013a, 2013b). Meanwhile, the downregulation of EUKARYOTIC INITIATION FACTOR 4B2 (eIF4B2) protein suggested the inhibited regulation of the translation initiation stage (Dutt et al., 2015). The *SNS-D mutant with the* increased expression level of the eIF4B2 gene resulted in spontaneous necrotic spots, DNA fragmentation, increased caspase activity, and ultimately programmed cell death (Gaussand et al., 2011). The suppressed RNA-binding protein eIF4B2 in the current study could have repressed the helicase activity of eIF4A and the eIF4E component of the eIF4F complex (Rogers et al., 2001) but might be beneficial in influencing mRNA discrimination during translation initiation as well as preventing programmed cell death (Mayberry et al., 2009; Rogers et al., 2001).

Our study further suggested the impaired SCF(TIR1) mediated protein degradation SUPPRESSOR OF THE G2 ALLELE OF SKP1 A (SGT1A). Despite the probable inhibition of $SCF^{TIR1}$ and serine protease degradation, lumichrome treatment triggered an increase in PROTEASOME REGULATOR1 (PTRE1), the proteasome related to ubiquitin protein degradation. PTRE1 is a positive regulator of the 26S proteasome through fine-tuning the homeostasis of Aux/IAA repressor proteins, thus modifying auxin activity (Yang et al., 2016). In that regard, a reduction in PTRE1 function is responsible for auxin-mediated proteasome suppression (Thulasi Devendrakumar et al., 2019). Cysteine proteases are believed to speed up reconfiguring the chloroplast proteome. However, inhibiting these proteases has been found to decelerate chloroplast protein degradation and, instead, activate photosynthetic gene expression and signalling between chloroplast and nucleus. This, in turn, enhances stress tolerance traits (Alomrani et al., 2021).

The high abundance of CHLOROPLAST HEAT SHOCK PROTEIN 70-1 (cpHSC70-1) and CHAPERONIN 20 (CPN20) suggests that lumichrome is involved in the prevention of protein aggregation and enables the disaggregation of cytotoxic aggregates. Lumichrome could have achieved this by binding to and stabilizing partially or unfolded protein polypeptides while also assisting in the unfolding of misfolded proteins (Finka et al., 2016; Flores-Pérez and Jarvis, 2013; Latijnhouwers et al., 2010; Liberek et al., 2008). This could have improved protein import into chloroplasts (Rochaix, 2022; Su and Li, 2010) and

contributed in maintaining chloroplast structure and functions (Su and Li, 2010). In *Physcomitrium patens* and *A. thaliana*, the disruption of cpHSC70-1 resulted in loss of chloroplast import and processing with eventual white seedling phenotype and seedling lethality (Cline and Dabney-Smith, 2008; Ding et al., 2022; Shipman-Roston et al., 2010). Interestingly, an inverse response was observed for the proteins related to the translocon in the outer envelope of chloroplasts (TOC) and translocon in the inner envelope of chloroplasts (TIC). These complexes play critical roles in delivering nuclear-encoded proteins into chloroplasts (Fukazawa et al., 2020; Kim et al., 2023; Lee and Hwang, 2021). These include the suppression of the TRANSLOCON AT THE INNER ENVELOPE MEMBRANE OF CHLOROPLASTS 62 (TIC62) and the TRANSLOCON AT THE OUTER ENVELOPE MEMBRANE OF CHLOROPLASTS 159 (TOC159). The *TOC159* gene is highly abundant in photosynthetic green tissues and serves as the primary protein import receptor for photosynthesis-associated proteins (Bauer et al., 2000).On the other hand, a study of *A. thaliana* (Benz et al., 2009), suggested that TIC62 acts as a redox sensor for the complex due to its redox-dependent movement between the envelope and stroma, as well as its specific interaction with the photosynthetic protein ferredoxin-NADP(H) oxidoreductase (FNR). In that regard, the high abundance of cpHSC70-1 and CPN20 following lumichrome treatment may have played a significant role in protein importation during an impaired TIC/TOC complex.

### 4.4. Hormone signalling regulation in response to lumichrome treatment

Lumichrome-related decreased transcriptional regulation of jasmonate biosynthesis has been previously reported in *A. thaliana*. This was shown through downregulating *LIPOXYGENASE 2, 3,* and *6* (*LOX2, LOX3, LOX6*) gene expression. Additionally, the downregulation of *JACALIN-RELATED LECTIN 34* (*JAL34*) and *JASMONATE RESPONSIVE 1* (*JR1*) gene expression was also observed (Pholo et al., 2018). This altogether suggested a substantive role of lumichrome in delayed leaf senescence through the suppression of the effects of MeJa, such as chlorophyll loss and decreases in RuBisCO and photosynthesis (Pholo et al., 2018). In addition to the previously reported suppression of the jasmonate-related protein, our study demonstrated a decrease in the expression of the Jasmonic acid (JA) biosynthesis-related proteins, specifically the ALLENE OXIDE CYCLASE 2 (AOC2). We also observed an opposing response in which the reduced AOC2 jasmonate-related protein was inversely correlated with the increased abundance of the ABSCISCIC RESPONSE PROTEIN (ABR) protein. Both the AOC2 and the ABR proteins have been reported to play an essential role in the leaf senescence response mechanism under environmental stress conditions in *A. thaliana* (Hu et al., 2017; Su et al., 2016). Thus, an increase in the expression level of the *AOC2* gene positively correlated with JA-promoted leaf senescence (He et al., 2002), while the *abr* knockout mutant revealed that ABR is involved in dark-induced leaf senescence in *A. thaliana* (Huang et al., 2022). Therefore, we propose that the downregulated AOC2 protein and the high abundance of ABR could have delayed both light and dark-induced leaf senescence. The expression of these proteins with a concomitant increase in chlorophyll *a* and *b* further suggested the enhanced prevention of chlorophyll degradation and protection of photosynthesis proteins from aggregation caused by light deprivation (Su et al., 2016). These probable jasmonate-related signals of delayed leaf senescence might have contributed to the promotion of optimal light absorption, energy transformation, and electron transfer capacity of active PSII reaction (Grübler et al., 2021; Papuga et al., 2010).

## 5. Conclusions

Proteomic analysis indicated that the lumichrome promotes *A. thaliana* growth by enhancing multiple aspects of the photosynthetic process and altering carbon partitioning away from starch synthesis to favour sucrose and reducing sugars. The promoted photosynthesis rate following lumichrome treatment was probably due to an increased stomal conductivity and transpiration rate that may have subsequently enhanced the $CO_2$ uptake.

The increase in chlorophyll a and b suggests better solar energy capture and absorption, which likely helped move electrons to the photosynthetic reaction centre. Proteomic profiling showed that the improved photosynthesis rate could be attributed to an abundance of proteins responsible for regulating the four major protein complexes involved in photosynthesis: photosystem I (PSI), photosystem II (PSII), cytochrome B6F, and ATPase. The high abundance of PSBQ-1 and PSBQ-2 likely enhanced the OEC required for PSII assembly, stability, and photoautotrophic growth. The abundance of these two luminal PSBQ proteins may have compensated for the N-terminal functional defect of PSBP in ensuring PSII stability. The low abundance of PSAE1 and a lack of light green pigmentation might be due to an efficient cyclic electron transport of PSI and dissipation of excess heat through the NPQ mechanism, promoting an effective photosynthesis rate.

In addition to the cyclic electron transport, lumichrome treatment suggested that the high abundance of ATPD enhanced linear electron transport with enhanced carbon assimilation and photosynthesis efficiency. The ability to counteract the production of singlet oxygen ($^1O2$) at photosystem (PS) II and superoxide anion ($O^{\cdot -2}$) at PSI in lumichrome-treated plants could be induced by the high abundance of TRX-M1, TRX-M4, plastid PRX-IIE, and the cytosolic Ascorbate peroxidase 1 (APX1) proteins, thereby improving $CO_2$ assimilation rate and plant growth.

In addition, treatment with lumichrome suggested enhanced carbon partitioning metabolism related to FBA8, possibly through sucrose biosynthesis. This process provided the cell with ATP and NADH for plant growth. Lumichrome treatment also increased Proteasome regulator1 (PTRE1), the proteasome related to ubiquitin protein degradation. In contrast, enhanced protein folding was suggested by the rise in cpHSC70-1 and the co-chaperone CPN20 proteins. The high abundance cpHSC70-1 suggested improved chloroplast import and processing, compensating for the impaired TIC/TOC complex.

Regarding hormonal signalling, our study proposes that the underrepresentation of the AOC2 protein and the high abundance of ABR protein may have significantly delayed leaf senescence, including the ABR gene's dark-induced leaf senescence.

Altogether, the proteome profiling of lumichrome-treated *A. thaliana* has uncovered various regulatory mechanisms that could have a profound impact on future research and applications in the field of plant biology and biotechnology. However, future research involving mutants or transgenic plants to either reduce or overexpress these photosynthetic and other identified potential metabolism-related candidate genes will help confirm the proposed lumichrome-associated modes of action.

## Data availability

The mass spectrometry proteomics data have been deposited to the ProteomeXchange Consortium via the PRIDE [1] partner repository with the dataset identifier PXD014006.

## Declaration of competing interest

The authors declare that the research was conducted in the absence of any commercial or financial relationships that could be construed as potential conflicts of interest.

## CRediT authorship contribution statement

**Motlalepula Pholo-Tait:** Conceptualization, Methodology, Investigation, Formal analysis, Writing – original draft. **Waltraud X. Schulze:** Investigation, Formal analysis. **Saleh Alseekh:** Investigation, Formal analysis. **Alex J. Valentine:** Formal analysis. **Nicholas C. Le Maitre:** Writing – review & editing. **James R. Lloyd:** Conceptualization, Methodology, Supervision, Writing – review & editing. **Jens Kossmann:** Conceptualization, Methodology, Supervision, Writing – review & editing, Funding acquisition. **Paul N. Hills:** Conceptualization, Methodology, Supervision, Writing – review & editing, Project administration.

## Funding

This research was funded by the National Research Foundation (SARChi Research Chair "Genetic tailoring of biopolymers") of South Africa.

## Acknowledgement

This manuscript is dedicated to the memory of Prof Jens Kossmann (1963–2023)

## Supplementary materials

Supplementary material associated with this article can be found, in the online version, at doi:10.1016/j.sajb.2024.07.036.

## References

Alomrani, S., Kunert, K.J., Foyer, C.H., 2021. Papain-like cysteine proteases are required for the regulation of photosynthetic gene expression and acclimation to high light stress. J. Exp. Bot. 72, 3441–3454. https://doi.org/10.1093/jxb/erab101.

Backhausen, J.E., Vetter, S., Baalmann, E., Kitzmann, C., Scheibe, R., 1998. NAD-dependent malate dehydrogenase and glyceraldehyde 3-phosphate dehydrogenase isoenzymes play an important role in dark metabolism of various plastid types. Planta 205, 359–366. https://doi.org/10.1007/s004250050331.

Bauer, J., Chen, K., Hiltbunner, A., Wehrli, E., Eugster, M., Schnell, D., Kessler, F., 2000. The major protein import receptor of plastids is essential for chloroplast biogenesis. Nature 403, 203–207. https://doi.org/10.1038/35003214.

Benjamini, Y., Hochberg, Y., 1995. Controlling the false discovery rate: a practical and powerful approach to multiple testing. J. R. Stat. Soc.. https://doi.org/10.2307/2346101.

Benz, J.P., Stengel, A., Lintala, M., Lee, Y.H., Weber, A., Philippar, K., Gügel, I.L., Kaieda, S., Ikegami, T., Mulo, P., Soll, J., Bölter, B., 2009. Arabidopsis Tic62 and ferredoxin-NADP(H) oxidoreductase form light-regulated complexes that are integrated into the chloroplast redox poise. Plant Cell 21, 3965–3983. https://doi.org/10.1105/tpc.109.069815.

Bradford, M.M., 1976. A rapid and sensitive method for the quantitation of microgram quantities of protein using the principle of protein dye binding. Anal. Biochem. 72, 248–254. https://doi.org/10.1016/0003-2697(76)90527-3.

Cai, B., Li, Q., Xu, Y., Yang, L., Bi, H., Ai, X., 2016. Genome-wide analysis of the fructose 1,6-bisphosphate aldolase (FBA) gene family and functional characterization of *FBA7* in tomato. Plant Physiol. Biochem. 108, 251–265. https://doi.org/10.1016/j.plaphy.2016.07.019.

Caspar, T., Huber, S.C., Somerville, S., 1985. Alterations in growth, photosynthesis, and respiration in a starchless mutant of Arabidopsis thaliana (L.) deficient in chloroplast phosphoglucomutase activity. Plant Physiol. 79, 11–17. https://doi.org/10.1104/pp.79.1.11.

Caspy, I., Nelson, N., 2018. Structure of the plant photosystem I. Biochem. Soc. Trans.. https://doi.org/10.1042/BST20170299.

Cejudo, F.J., González, M.C., Pérez-Ruiz, J.M., 2021. Redox regulation of chloroplast metabolism. Plant Physiol. 186, 9–21. https://doi.org/10.1093/plphys/kiaa062.

Chaiwongsar, S., Strohm, A.K., Su, S.-H., Krysan, P.J., 2012. Genetic analysis of the *Arabidopsis* protein kinases MAP3K 1 and MAP3K 2 indicates roles in cell expansion and embryo development. Front. Plant Sci. 3, 1–10. https://doi.org/10.3389/fpls.2012.00228.

Cho, M.H., Jang, A., Bhoo, S.H., Jeon, J.S., Hahn, T.R., 2012. Manipulation of triose phosphate/phosphate translocator and cytosolic FRUCTOSE-1,6-BISPHOSPHATASE, the key components in photosynthetic sucrose synthesis, enhances the source capacity of transgenic *Arabidopsis* plants. Photosynth. Res. 111, 261–268. https://doi.org/10.1007/s11120-012-9720-2.

Cline, K., Dabney-Smith, C., 2008. Plastid protein import and sorting: different paths to the same compartments. Curr. Opin. Plant Biol.. https://doi.org/10.1016/j.pbi.2008.10.008.

Collin, V., Issakidis-Bourguet, E., Marchand, C., Hirasawa, M., Lancelin, J.M., Knaff, D.B., Miginiac-Maslow, M., 2003. The *Arabidopsis* plastidial thioredoxins. New functions and new insights into specificity. J. Biol. Chem. 278, 23747–23752. https://doi.org/10.1074/jbc.M302077200.

Cox, J., Mann, M., 2011. Quantitative, high-resolution proteomics for data-driven systems biology. Annu. Rev. Biochem. 80, 273–299. https://doi.org/10.1146/annurev-biochem-061308-093216.

Cox, J., Mann, M., 2008. MaxQuant enables high peptide identification rates, individualized p.p.b.-range mass accuracies and proteome-wide protein quantification. Nat. Biotechnol. 26, 1367–1372. https://doi.org/10.1038/nbt.1511.

Ding, F., Li, F., Zhang, B., 2022. A plastid-targeted heat shock cognate 70-kDa protein confers osmotic stress tolerance by enhancing ROS scavenging capability. Front. Plant Sci. 13, 1012145. https://doi.org/10.3389/fpls.2022.1012145.

Dogra, V., Duan, J., Lee, K.P., Kim, C., 2019. Impaired PSII proteostasis triggers a UPR-like response in the *var2* mutant of Arabidopsis. J. Exp. Bot. 70, 3077–3088. https://doi.org/10.1093/jxb/erz151.

Dreyer, A., Treffon, P., Basiry, D., Jozefowicz, A.M., Matros, A., Mock, H.P., Dietz, K.J., 2021. Function and regulation of chloroplast peroxiredoxin IIe. Antioxidants 10. https://doi.org/10.3390/antiox10020152.

Dutt, S., Parkash, J., Mehra, R., Sharma, N., Singh, B., Raigond, P., Joshi, A., Chopra, S., Singh, B.P., 2015. Translation initiation in plants: roles and implications beyond protein synthesis. Biol. Plant.. https://doi.org/10.1007/s10535-015-0517-y.

Ermakova, M., Heyno, E., Woodford, R., Massey, B., Birke, H., Von Caemmerer, S., 2022. Enhanced abundance and activity of the chloroplast ATP synthase in rice through the overexpression of the AtpD subunit. J. Exp. Bot. 73, 6891–6901. https://doi.org/10.1093/jxb/erac320.

Finka, A., Mattoo, R.U.H., Goloubinoff, P., 2016. Experimental milestones in the discovery of molecular chaperones as polypeptide unfolding enzymes. Annu. Rev. Biochem. 85, 715–742. https://doi.org/10.1146/annurev-biochem-060815-014124.

Flores-Pérez, Ú., Jarvis, P., 2013. Molecular chaperone involvement in chloroplast protein import. Biochim. Biophys. Acta - Mol. Cell Res.. https://doi.org/10.1016/j.bbamcr.2012.03.019.

Fromme, P., Melkozernov, A., Jordan, P., Krauss, N., 2003. Structure and function of photosystem I: interaction with its soluble electron carriers and external antenna systems. FEBS Lett. 27, 40–44. https://doi.org/10.1016/S0014-5793(03)01124-4.

Fukazawa, H., Tada, A., Richardson, L.G.L., Kakizaki, T., Uehara, S., Ito-Inaba, Y., Inaba, T., 2020. Induction of TOC and TIC genes during photomorphogenesis is mediated primarily by cryptochrome 1 in *Arabidopsis*. Sci. Rep 10. https://doi.org/10.1038/s41598-020-76939-w.

Gao, Z.P., Chen, G.X., Yang, Z.N., 2012. Regulatory role of *Arabidopsis pTAC14* in chloroplast development and plastid gene expression. Plant Signal. Behav.. https://doi.org/10.4161/psb.21618.

Gaussand, G.M.D.J.M., Jia, Q., Van Der Graaff, E., Lamers, G.E.M., Fransz, P.F., Hooykaas, P.J.J., De Pater, S., 2011. Programmed cell death in the leaves of the *Arabidopsis* spontaneous necrotic spots (*sns-D*) mutant correlates with increased expression of the eukaryotic translation initiation factor eif4b2. Front. Plant Sci 2, 9. https://doi.org/10.3389/fpls.2011.00009.

Gouws, L.M., 2009. The Molecular analysis of the Effects of Lumichrome as a Plant Growth Promoting Substance by Liezel Michelle Gouws. Stellenbosch University.

Gouws, L.M., Botes, E., Wiese, A.J., Trenkamp, S., Torres-Jerez, I., Tang, Y., Hills, P.N., Usadel, B., Lloyd, J.R., Fernie, A.R., Kossmann, J., van der Merwe, M.J., 2012. The plant growth promoting substance, lumichrome, mimics starch, and ethylene-associated symbiotic responses in lotus and tomato roots. Front. Plant Sci. 3, 1–20. https://doi.org/10.3389/fpls.2012.00120.

Grübler, B., Cozzi, C., Pfannschmidt, T., 2021. A core module of nuclear genes regulated by biogenic retrograde signals from plastids. Plants 10, 296. https://doi.org/10.3390/plants10020296.

Hald, S., Pribil, M., Leister, D., Gallois, P., Johnson, G.N., 2008. Competition between linear and cyclic electron flow in plants deficient in Photosystem I. Biochim. Biophys. Acta - Bioenerg. 1777, 1173–1183. https://doi.org/10.1016/j.bbabio.2008.04.041.

Harb, J., Alseekh, S., Tohge, T., Fernie, A.R., 2015. Profiling of primary metabolites and flavonols in leaves of two table grape varieties collected from semiarid and temperate regions. Phytochemistry 117, 444–455. https://doi.org/10.1016/j.phytochem.2015.07.013.

He, Y., Fukushige, H., Hildebrand, D.F., Gan, S., 2002. Evidence supporting a role of jasmonic acid in *Arabidopsis* leaf senescence. Plant Physiol. 128, 876–884. https://doi.org/10.1104/pp.010843.

Heise, R., Arrivault, S., Szecowka, M., Tohge, T., Nunes-Nesi, A., Stitt, M., Nikoloski, Z., Fernie, A.R., 2014. Flux profiling of photosynthetic carbon metabolism in intact plants. Nat. Protoc. 9, 1803–1824. https://doi.org/10.1038/nprot.2014.115.

Hu, Y., Jiang, Y., Han, X., Wang, H., Pan, J., Yu, D., 2017. Jasmonate regulates leaf senescence and tolerance to cold stress: crosstalk with other phytohormones. J. Exp. Bot. 68, 1361–1369. https://doi.org/10.1093/jxb/erx004.

Huang, P., Li, Z., Guo, H., 2022. New advances in the regulation of leaf senescence by classical and peptide hormones. Front. Plant Sci.. https://doi.org/10.3389/fpls.2022.923136.

Ifuku, K., Yamamoto, Y., Ono, T.-A., Ishihara, S., Sato, F., 2005. PsbP protein, but not PsbQ protein, is essential for the regulation and stabilization of photosystem II in higher plants. Plant Physiol. 139, 1175–1184. https://doi.org/10.1104/pp.105.068643.

Ihnatowicz, A., Pesaresi, P., Leister, D., 2007. The E subunit of photosystem I is not essential for linear electron flow and photoautotrophic growth in *Arabidopsis thaliana*. Planta 226, 889–895. https://doi.org/10.1007/s00425-007-0534-y.

Inomata, T., Baslam, M., Masui, T., Koshu, T., Takamatsu, T., Kaneko, K., Pozueta-Romero, J., Mitsui, T., 2018. Proteomics analysis reveals non-controlled activation of photosynthesis and protein synthesis in a rice npp1 mutant under high temperature and elevated $CO_2$ conditions. Int. J. Mol. Sci. 19, 2655. https://doi.org/10.3390/ijms19092655.

Jahns, P., Holzwarth, A.R., 2012. The role of the xanthophyll cycle and of lutein in photoprotection of photosystem II. Biochim. Biophys. Acta - Bioenerg.. https://doi.org/10.1016/j.bbabio.2011.04.012.
Kakiuchi, S., Uno, C., Ido, K., Nishimura, T., Noguchi, T., Ifuku, K., Sato, F., 2012. The PsbQ protein stabilizes the functional binding of the PsbP protein to photosystem II in higher plants. Biochim. Biophys. Acta - Bioenerg. 1817, 1346–1351. https://doi.org/10.1016/j.bbabio.2012.01.009.
Kanazawa, A., Kramer, D.M., 2002. In vivo modulation of nonphotochemical exciton quenching (NPQ) by regulation of the chloroplast ATP synthase. Proc. Natl. Acad. Sci. U.S.A. 99, 12789–12794. https://doi.org/10.1073/pnas.182427499.
Kato, Y., Miura, E., Ido, K., Ifuku, K., Sakamoto, W., 2009. The variegated mutants lacking chloroplastic FtsHs are defective in D1 degradation and accumulate reactive oxygen species. Plant Physiol. 151, 1790–1801. https://doi.org/10.1104/pp.109.146589.
Kekulandara, D.N., Nagi, S., Seo, H., Chow, C.S., Ahn, Y.H., 2018. Redox-Inactive peptide disrupting *Trx1-Ask1* interaction for selective activation of stress signaling. Biochemistry 57, 772–780. https://doi.org/10.1021/acs.biochem.7b01083.
Khan, W., Prithiviraj, B., Smith, D.L., 2008. Nod factor [Nod Bj V (C18:1, MeFuc)] and lumichrome enhance photosynthesis and growth of corn and soybean. J. Plant Physiol. 165, 1342–1351. https://doi.org/10.1016/j.jplph.2007.11.001.
Kim, D.B., Na, C., Hwang, I., Lee, D.W., 2023. Understanding protein translocation across chloroplast membranes: translocons and motor proteins. J. Integr. Plant Biol. 65, 408–416. https://doi.org/10.1111/jipb.13385.
Koch, K., 2004. Sucrose metabolism: regualtory mechanisms and pivotal roles in sugar sensing and plant development. Curr. Opin. Plant Biol. 7, 235–246. https://doi.org/10.1016/j.pbi.2004.03.014.
Kubota-Kawai, H., Mutoh, R., Shinmura, K., Sétif, P., Nowaczyk, M.M., Rögner, M., Ikegami, T., Tanaka, H., Kurisu, G., 2018. X-ray structure of an asymmetrical trimeric ferredoxin-photosystem I complex. Nat. Plants 4, 218–224. https://doi.org/10.1038/s41477-018-0130-0.
Kusumi, K., Hirotsuka, S., Kumamaru, T., Iba, K., 2012. Increased leaf photosynthesis caused by elevated stomatal conductance in a rice mutant deficient in *SLAC1*, a guard cell anion channel protein. J. Exp. Bot. 63, 5635–5644. https://doi.org/10.1093/jxb/ers216.
Lambrecht, J.A., Schmitz, G.E., Downs, D.M., 2013. RidA proteins prevent metabolic damage inflicted by PLP-dependent dehydratases in all domains of life. MBio 4, e00033. https://doi.org/10.1128/mBio.00033-13 -13.
Latijnhouwers, M., Xu, X.M., Møller, S.G., 2010. *Arabidopsis* stromal 70-kDa heat shock proteins are essential for chloroplast development. Planta 232, 567–578. https://doi.org/10.1007/s00425-010-1192-z.
Leakey, A.D.B., Ainsworth, E.A., Bernacchi, C.J., Rogers, A., Long, S.P., Ort, D.R., 2009. Elevated $CO_2$ effects on plant carbon, nitrogen, and water relations: six important lessons from FACE. J. Exp. Bot. 60, 2859–2876. https://doi.org/10.1093/jxb/erp096.
Lee, D.W., Hwang, I., 2021. Understanding the evolution of endosymbiotic organelles based on the targeting sequences of organellar proteins. New Phytol.. https://doi.org/10.1111/nph.17167.
Leister, D., 2003. Chloroplast research in the genomic age. Trends Genet. 19, 47–56. https://doi.org/10.1016/S0168-9525(02)00003-3.
Liberek, K., Lewandowska, A., Zięłkiewicz, S., 2008. Chaperones in control of protein disaggregation. EMBO 27, 328–335. https://doi.org/10.1038/sj.emboj.7601970.
Lin, T.-P., Caspar, T., Somerville, C.R., Preiss, J., 1988. A starch deficient mutant of *Arabidopsis thaliana* with low ADPglucose pyrophosphorylase activity lacks one of the two subunits of the enzyme. Plant Physiol 88, 1175–1181. https://doi.org/10.1104/pp.88.4.1175.
Lisec, J., Schauer, N., Kopka, J., Willmitzer, L., Fernie, A., 2006. Gas chromatography mass spectrometry-based metabolite profiling in plants. Nat. Protoc. 1, 387–396. https://doi.org/10.1038/nprot.2006.59.
Liu, J., Last, R.L., 2017. A chloroplast thylakoid lumen protein is required for proper photosynthetic acclimation of plants under fluctuating light environments. Proc. Natl. Acad. Sci. U.S.A. 114, E8110–E8117. https://doi.org/10.1073/pnas.1712206114.
Lu, W., Tang, X., Huo, Y., Xu, R., Qi, S., Huang, J., Zheng, C., Wu, C.A., 2012. Identification and characterization of fructose 1,6-bisphosphate aldolase genes in *Arabidopsis* reveal a gene family with diverse responses to abiotic stresses. Gene 503, 65–74. https://doi.org/10.1016/j.gene.2012.04.042.
Luedemann, A., Von Malotky, L., Erban, A., Kopka, J., 2012. TagFinder: preprocessing software for the fingerprinting and the profiling of gas chromatography–mass spectrometry based metabolome analyses. Methods Mol. Biol. 860, 255–286. https://doi.org/10.1007/978-1-61779-594-7_16.
Manjunath, S., Lee, C.H., VanWinkle, P., Bailey-Serres, J., 1998. Molecular and biochemical characterization of cytosolic phosphoglucomutase in maize. Expression during development and in response to oxygen deprivation. Plant Physiol. 117, 997–1006. https://doi.org/10.1104/Pp.117.3.997.
Matiru, V., Dakora, F., 2005. Xylem transport and shoot accumulation of lumichrome, a newly recognized rhizobial signal, alters root respiration, stomatal conductance, leaf transpiration and photosynthetic rates in legumes and cereals. New Phytol 165, 847–855. https://doi.org/10.1111/j.1469-8137.2004.01254.x.
Matiru, V.N., Dakora, F.D., 2005. The rhizosphere signal molecule lumichrome alters seedling development in both legumes and cereals. New Phytol. 166, 439–444. https://doi.org/10.1111/j.1469-8137.2005.01344.x.
Matthews, J.S.A., Lawson, T., 2018. Climate change and stomatal physiology. Annu. Plant Rev. 713–752. https://doi.org/10.1002/9781119312994.apr0667.
Mauceri, A., Puccio, G., Faddetta, T., Abbate, L., Polito, G., Caldiero, C., Renzone, G., Lo Pinto, M., Alibrandi, P., Vaccaro, E., Abenavoli, M.R., Scaloni, A., Sunseri, F., Cavalieri, V., Palumbo Piccionello, A., Gallo, G., Mercati, F., 2024. Integrated omics approach reveals the molecular pathways activated in tomato by *Kocuria rhizophila*, a soil plant growth-promoting bacterium. Plant Physiol. Biochem. 210, 108609. https://doi.org/10.1016/j.plaphy.2024.108609.
Mayberry, L.K., Leah Allen, M., Dennis, M.D., Browning, K.S., 2009. Evidence for variation in the optimal translation initiation complex: plant eIF4B, eIF4F, and eIF(iso)4F differentially promote translation of mRNAs. Plant Physiol. 150, 1844–1854. https://doi.org/10.1104/pp.109.138438.
Müller-Röber, B., Sonnewald, U., Willmitzer, L., 1992. Inhibition of the ADP-glucose pyrophosphorylase in transgenic potatoes leads to sugar-storing tubers and influences tuber formation and expression of tuber storage protein genes. EMBO J. 11, 1229–1238.
Munekage, Y., Hojo, M., Meurer, J., Endo, T., Tasaka, M., Shikanai, T., 2002. PGR5 is involved in cyclic electron flow around photosystem I and is essential for photoprotection in *Arabidopsis*. Cell 110, 361–371. https://doi.org/10.1016/S0092-8674(02)00867-X.
Muñoz-Bertomeu, J., Cascales-Miñana, B., Mulet, J.M., Baroja-Fernández, E., Pozueta-Romero, J., Kuhn, J.M., Segura, J., Ros, R., 2009. Plastidial glyceraldehyde-3-phosphate dehydrogenase deficiency leads to altered root development and affects the sugar and amino acid balance in *Arabidopsis*. Plant Physiol. 151, 541–558. https://doi.org/10.1104/pp.109.143701.
Naake, T., Zhu, F., Alseekh, S., Scossa, F., Perez de Souza, L., Borghi, M., Brotman, Y., Mori, T., Nakabayashi, R., Tohge, T., Fernie, A.R., 2024. Genome-wide association studies identify loci controlling specialized seed metabolites in *Arabidopsis*. Plant Physiol. 194, 1705–1721. https://doi.org/10.1093/plphys/kiad511.
Næsted, H., Holm, A., Jenkins, T., Nielsen, H.B., Harris, C.A., Beale, M.H., Andersen, M., Mant, A., Scheller, H., Camara, B., Mattsson, O., Mundy, J., 2004. *Arabidopsis VARIEGATED 3* encodes a chloroplast-targeted, zinc-finger protein required for chloroplast and palisade cell development. J. Cell Sci. 117, 4804–4818. https://doi.org/10.1242/jcs.01360.
Nelson, N., Yocum, C.F., 2006. Structure and function of photosystems I and II. Annu. Rev. Plant Biol. 57, 521–565. https://doi.org/10.1146/annurev.arplant.57.032905.105350.
Niehaus, T.D., Nguyen, T.N.D., Gidda, S.K., ElBadawi-Sidhu, M., Lambrecht, J.A., McCarty, D.R., Downs, D.M., Cooper, A.J.L., Fiehn, O., Mullen, R.T., Hanson, A.D., 2014. *Arabidopsis* and maize RidA proteins preempt reactive enamine/imine damage to branched-chain amino acid biosynthesis in plastids. Plant Cell 26, 3010–3022. https://doi.org/10.1105/tpc.114.126854.
Okegawa, Y., Motohashi, K., 2015. Chloroplastic thioredoxin m functions as a major regulator of Calvin cycle enzymes during photosynthesis *in vivo*. Plant J. 84, 900–913. https://doi.org/10.1111/tpj.13049.
Olsen, J.V., Ong, S.E., Mann, M., 2004. Trypsin cleaves exclusively C-terminal to arginine and lysine residues. Mol. Cell. Proteom. 3, 608–614. https://doi.org/10.1074/mcp.T400003-MCP200.
Papuga, J., Hoffmann, C., Dieterle, M., Moes, D., Moreau, F., Tholl, S., Steinmetz, A., Thomas, C., 2010. *Arabidopsis* LIM proteins: a family of actin bundlers with distinct expression patterns and modes of regulation. Plant Cell 22, 3034–3052. https://doi.org/10.1105/tpc.110.075960.
Pfalz, J., Liere, K., Kandlbinder, A., Dietz, K.J., Oelmüller, R., 2006. pTAC2,-6, and-12 are components of the transcriptionally active plastid chromosome that are required for plastid gene expression. Plant Cell 18, 176–197. https://doi.org/10.1105/tpc.105.036392.
Phillips, D.A., Joseph, C.M., Yang, G.P., Martinez-Romero, E., Sanborn, J.R., Volpin, H., 1999. Identification of lumichrome as a *sinorhizobium* enhancer of alfalfa root respiration and shoot growth. Proc. Natl. Acad. Sci. U.S.A. 96, 12275–12280. https://doi.org/10.1073/pnas.96.22.12275.
Pholo, M., Coetzee, B., Maree, H.J., Young, P.R., Lloyd, J.R., Kossmann, J., Hills, P.N., 2018. Cell division and turgor mediate enhanced plant growth in *Arabidopsis* plants treated with the bacterial signalling molecule lumichrome. Planta 248, 477–488. https://doi.org/10.1007/s00425-018-2916-8.
Pogson, B.J., Albrecht, V., 2011. Genetic dissection of chloroplast biogenesis and development: An overview. Plant Physiol. 155, 1545–1551. https://doi.org/10.1104/pp.110.170365.
Rast, A., Heinz, S., Nickelsen, J., 2015. Biogenesis of thylakoid membranes. Biochim. Biophys. Acta. https://doi.org/10.1016/j.bbabio.2015.01.007.
Rochaix, J.D., 2022. Chloroplast protein import machinery and quality control. FEBS 289, 6908–6918. https://doi.org/10.1111/febs.16464.
Rogers, G.W., Richter, N.J., Lima, W.F., Merrick, W.C., 2001. Modulation of the helicase activity of eIF4A by eIF4B, eIF4H, and eIF4F. J. Biol. Chem. 276. https://doi.org/10.1074/jbc.M100157200.
Rott, M., Martins, N.F., Thiele, W., Lein, W., Bock, R., Kramer, D.M., Schöttlera, M.A., 2011. ATP synthase repression in tobacco restricts photosynthetic electron transport, $CO_2$ assimilation, and plant growth by overacidification of the thylakoid lumen. Plant Cell 23, 304–321. https://doi.org/10.1105/tpc.110.079111.
Rühle, T., Leister, D., 2015. Assembly of F1F0-ATP synthases. Biochim. Biophys. Acta - Bioenerg.. https://doi.org/10.1016/j.bbabio.2015.02.005.
Sakamoto, W., Miyagishima, S., Jarvis, P., 2008. Chloroplast biogenesis: control of plastid development, protein import, division and inheritance, *The Arabidopsis* Book/American Society of Plant Biologists. Arabidopsis Book. 2008; 6, e0110. https://doi.org/10.1199/tab.0110.
Sakamoto, W., Tamura, T., Hanba-Tomita, Y., Sodmergen, Murata, M., 2002. The *VAR1 locus* of *Arabidopis* encodes a choloroplastic FtsH and is responsible for leaf variegation in the mutant alleles. Genes Cells 7, 769–780. https://doi.org/10.1046/j.1365-2443.2002.00558.x.
Shipman-Roston, R.L., Ruppel, N.J., Damoc, C., Phinney, B.S., Inoue, K., 2010. The significance of protein maturation by plastidic type I signal peptidase 1 for thylakoid development in *Arabidopsis* chloroplasts. Plant Physiol. 152, 1297–1308. https://doi.org/10.1104/pp.109.151977.
Skotnicová, P., Srivastava, A., Aggarwal, D., Talbot, J., Karlínová, I., Moos, M., Mareš, J., Bučinská, L., Koník, P., Šimek, P., Tichý, M., Sobotka, R., 2023. A thylakoid biogenesis BtpA protein is required for the initial step of tetrapyrrole biosynthesis in *cyanobacteria*. New Phytol. 241, 1236–1249. https://doi.org/10.1111/nph.19397.

Sreeharsha, R.V., Sekhar, K.M., Reddy, A.R., 2015. Delayed flowering is associated with lack of photosynthetic acclimation in Pigeon pea (*Cajanus cajan* L.) grown under elevated CO2. Plant Sci. 231, 82–93. https://doi.org/10.1016/j.plantsci.2014.11.012.

Stefan, T., Wu, X.N., Zhang, Y., Fernie, A., Schulze, W.X., 2022. Regulatory modules of metabolites and protein phosphorylation in arabidopsis genotypes with altered sucrose allocation. Front. Plant Sci. 13. https://doi.org/10.3389/fpls.2022.891405.

Su, M., Huang, G., Zhang, Q., Wang, X., Li, C., Tao, Y., Zhang, S., Lai, J., Yang, C., Wang, Y., 2016. The LEA protein, ABR, is regulated by ABI5 and involved in dark-induced leaf senescence in *Arabidopsis thaliana*. Plant Sci. 247. https://doi.org/10.1016/j.plantsci.2016.03.009.

Su, P.-H., Li, H., 2010. Stromal Hsp70 is important for protein translocation into pea and *Arabidopsis* chloroplasts. Plant Cell 22, 1516–1531. https://doi.org/10.1105/tpc.109.071415.

Sun, T., Rao, S., Zhou, X., Li, L., 2022. Plant carotenoids: recent advances and future perspectives. Mol. Hortic. 2, 3. https://doi.org/10.1186/s43897-022-00023-2.

Thulasi Devendrakumar, K., Copeland, C., Li, X., 2019. The proteasome regulator *PTRE1* contributes to the turnover of SNC1 immune receptor. Mol. Plant Pathol. 20, 1566–1573. https://doi.org/10.1111/mpp.12855.

Thuynsma, R., Kleinert, A., Kossmann, J., Valentine, A.J., Hills, P.N., 2016. The effects of limiting phosphate on photosynthesis and growth of *Lotus japonicus*. S. Afr. J. Bot. 104. https://doi.org/10.1016/j.sajb.2016.03.001.

Tikkanen, M., Aro, E.M., 2014. Integrative regulatory network of plant thylakoid energy transduction. Trends Plant Sci.. https://doi.org/10.1016/j.tplants.2013.09.003.

Toujani, W., Muñoz-Bertomeu, J., Flores-Tornero, M., Rosa-Téllez, S., Anoman, A.D., Alseekh, S., Fernie, A.R., Ros, R., 2013. Functional characterization of the plastidial 3-phosphoglycerate dehydrogenase family in *Arabidopsis*. Plant Physiol. 163, 1164–1178. https://doi.org/10.1104/pp.113.226720.

Varotto, C., Pesaresi, P., Meurer, J., Oelmüller, R., Steiner-Lange, S., Salamini, F., Leister, D., 2000. Disruption of the *Arabidopsis* photosystem I gene *psaE1* affects photosynthesis and impairs growth. Plant J. 22, 115–124. https://doi.org/10.1046/j.1365-313X.2000.00717.x.

Volpin, H., Phillips, D.a., 1998. Respiratory elicitors from *rhizobium meliloti* affect intact alfalfa roots. Plant Physiol. 116, 777–783. https://doi.org/10.1104/pp.116.2.777.

Wang, J., Lan, P., Gao, H., Zheng, L., Li, W., Schmidt, W., 2013. Expression changes of ribosomal proteins in phosphate- and iron-deficient *Arabidopsis* roots predict stress-specific alterations in ribosome composition. BMC Genomics 14. https://doi.org/10.1186/1471-2164-14-783.

Wang, P., Liu, J., Liu, B., Feng, D., Da, Q., Shu, S., Su, J., Zhang, Y., Wang, J., Wang, H., 2013. Evidence for a role of chloroplastic m-type thioredoxins in the biogenesis of photosystem II in *Arabidopsis*. Plant Physiol. 163, 1710–1728. https://doi.org/10.1104/pp.113.228353.

Wollman, F.A., Minai, L., Nechushtai, R., 1999. The biogenesis and assembly of photosynthetic proteins in thylakoid membranes. Biochim. Biophys. Acta - Bioenerg.. https://doi.org/10.1016/S0005-2728(99)00043-2.

Yang, B.-J., Han, X.-X., Yin, L.-L., Xing, M.-Q., Xu, Z.-H., Xue, H.-W., 2016. *Arabidopsis PROTEASOME REGULATOR1* is required for auxin-mediated suppression of proteasome activity and regulates auxin signalling. Nat. Commun. 7, 11388. https://doi.org/10.1038/ncomms11388.

Zauber, H., Schulze, W.X., 2012. Proteomics wants cRacker: automated standardized data analysis of LC-MS derived proteomic data. J. Proteome Res. 11, 5548–5555. https://doi.org/10.1021/pr300413v.

Zhu, D., Xiong, H., Wu, J., Zheng, C., Lu, D., Zhang, L., Xu, X., 2022. Protein targeting into the thylakoid membrane through different pathways. Front. Physiol.. https://doi.org/10.3389/fphys.2021.802057.

Zrenner, R., Krause, K.P., Apel, P., Sonnewald, U., 1996. Reduction of the cytosolic fructose-1,6-bisphosphatase in transgenic potato plants limits photosynthetic sucrose biosynthesis with no impact on plant growth and tuber yield. Plant J. 9, 671–681. https://doi.org/10.1046/j.1365-313X.1996.9050671.x.